"POLITEHNICA" UNIVERSITY from BUCHAREST
FACULTY of MATERIALS SCIENCE AND ENGINEERING
Doctoral School of Materials Engineering

PhD THESIS

ADVANCED RESEARCH ON OBTAINING THIN LAYERS WITH HIGH CORROSION RESISTANCE UNDER EXTREME CONDITIONS BY PVD METHODS

Scientific coordinators:

Prof.dr.eng. Cristian PREDESCU

Author:

Eng. Laurentiu Florin MOȘINOIU

EVALUATION BOARD OF THE PhD THESIS

President	***Prof. univ.dr.eng. Iulian Vasile ANTONIAC*** *Politehnica University of Bucharest*
Scientific coordinators	***Prof.dr.eng. Cristian PREDESCU*** *Politehnica University of Bucharest*
Scientific referees	***Prof. univ.dr.eng. Constantin BACIU*** *Gheorghe Asachi Technical University of Iași* ***CSI. Dr.eng. Radu Robert PITICESCU*** *I.N.C.D.M.N.R. din Pantelimon* ***Conf. univ.dr.eng. Andrei Constantin BERBECARU*** *Politehnica University of Bucharest*

Bucharest

2023

Summary

Keywords: oxide architectures, EB-PVD, stainless steel, electrochemical corrosion, scanning electron microscopy, X-ray diffraction.

Introduction

Physical vapour deposition (PVD) is a ubiquitous technique in today's world, widely used to manufacture thin films and improve the physical and chemical properties of materials. PVD is used extensively on an industrial scale and is combined with various methods to produce coatings with superior properties. Recent developments in nanoscience have made this technique increasingly useful for producing coatings with the desired microstructure and properties. Ongoing research and development of coatings and thin-film materials have evaluated their chemical and structural composition. This has led to the development of thin films and coatings that focus more on improving thin-film materials and determining optimal processing techniques to reduce the consumption of toxic substances. materials and reducing energy consumption during the processing of these materials.

As mentioned earlier, coatings have found a wide range of applications in both protective and decorative areas. However, the history of coatings shows that they have been used mainly for ornamental and decorative purposes. These coatings were made on walls and other ornaments to enhance their beauty and improve their functionality through artistic features and paintings. The coatings included edible natural polymer species such as earth pigments and synthetic oils.

PVD technology is very versatile, allowing the deposition of any type of inorganic material such as metals, alloys, compounds and mixtures, as well as some organic materials. Coatings are generally used to improve hardness, wear resistance and oxidation resistance. Thus, coatings are used in a wide range of applications such as: aerospace, automotive, surgical/medical, dyes and dies for all kinds of material processing, cutting tools, firearms, optics, watches, thin films (window tints, food packaging, etc.) and in the textile industry.

Corrosion protection of metals is a very important issue from an economic point of view and for its environmental implications. Corrosion prevents the widespread use of some interesting materials, such as magnesium alloys, in strategic applications such as transport and aerospace, and therefore many studies have been carried out to develop corrosion prevention strategies.

Based on these data, the research carried out in the PhD thesis aimed to obtain new oxide layer and multilayer architectures of Al_2O_3, ZrO2 and TiO_2, capable of responding to thermo-chemical corrosion stresses. The coatings were obtained using the EB-PVD electron beam vacuum deposition combinatorial method, with a particular focus on the development of new components for thermal equipment operating under extreme environmental conditions.

Thus, specific analyses and corrosion tests carried out under laboratory conditions revealed the chemical, morphological and structural characteristics of multilayer oxide architectures obtained by the EB-PVD method using scanning electron microscopy (SEM/ EDS), thin film adhesion testing by scratch test method and X-ray diffraction (XRD).

The thesis is structured in 9 chapters with 32 tables, 321 figures and 134 bibliographical references.

Chapter 1 entitled "**Survey of national and international research on the production of thin coatings in the field of the PhD topic**" contains general information from the literature on methods and techniques for obtaining TiO_2, ZrO_2 and Al_2O_3 based oxide coatings and their possible applications in industrial processes.

Chapter 2 entitled "**Mechanisms and forms of corrosion in steels**" contains information on the main forms of degradation or deterioration of some materials, usually metals, over time when, due to exposure to the environment oxygen and water lead to the formation of hydrated oxides, leading to the appearance of the corrosion process. This chapter also briefly describes the main types of corrosion occurring in steels and the importance of corrosion control of metals and alloys and their protection.

Chapter 3 called "**Research objectives and methodology**" contains information about the main objectives of the PhD thesis, the equipment used in the realization of oxide thin films layer and multilayer of Al_2O_3, ZrO_2 doped with rare earth oxides and TiO_2, as well as the research methodology and experimental design.

Chapter 4 entitled "**Thermodynamic modeling, obtaining and characterization of doped ZrO_2 nanostructured powde**r" includes, predictive thermodynamic calculations using specialized software as well as literature data; (HSC v.9-Outokumpu Finland, MATCALC-access on line to ENEA Rome network) and recent electronic database (NIST Phase Diagrams 2016-multiple license purchased from American Ceramic Society) as well as thermodynamic modeling by hydrothermal synthesis.

Chapter 5 entitled "**Obtaining and characterization of multilayer oxide architectures of type Al_2O_3; Y_2O_3-doped ZrO_2; $La_2Zr_2O_3$; Ce_2O_3, obtained by**

combinatorial EB-PVD method" covers the obtaining of three types of multilayer oxide coatings of type Al_2O_3, Y_2O_3-doped ZrO_2; $La_2Zr_2O_3$; Ce_2O_3, on 316L stainless steel substrate. Evaluation of the performance of the obtained oxide architectures was performed by carrying out tests on structure and morphology investigation by scanning electron microscopy (SEM - EDS) using X-ray diffraction (XRD) measurements. The determination of the adhesion of the obtained coatings was performed using the Test Scrach method, and the electrochemical corrosion studies were carried out at room temperature in an ASTM corrosion cell with a volume of 1L in the electrolyte solution used was NaCl of different concentrations, respectively 0.06M, 0.2M, 0.4M and 0.6M.

Chapter 6 entitled "**Obtaining and characterizing multilayer oxide architectures of type: NiCrAlY - Al_2O_3 and CeO_2 - doped ZrO_2 obtained by combinatorial EB-PVD method**" covers the obtaining of multilayer oxide architectures of the type Al_2O_3, CeO_2-doped ZrO_2, on austenitic 304L stainless steel substrate. The oxide coatings obtained were achieved by sandwiching a CeO2-doped ZrO_2 interlayer between the NiCrAlY steel layer and the Al_2O_3 surface layer. Investigation of the coating structure and morphology was carried out by scanning electron microscopy (SEM - EDS) and X-ray diffraction (XRD) measurements. Determination of the adhesion of the obtained coatings was performed using the Test Scrach method, and electrochemical corrosion studies were carried out at room temperature, in an ASTM corrosion cell with a volume of 1 L. The electrolyte solution used was H_2SO_4 1N, the experiments were carried out after 60 minutes of immersion of the electrodes in the electrolyte solution studied. The procedure by which the experiments were conducted was linear polarization.

Chapter 7 entitled "**Obtaining and characterization of experimental NiCrAlY - Al_2O_3 type experimental patterns on austenitic 316L stainless steel substrate by EB-PVD method intended for corrosion in molten Pb**" covers the obtaining of multilayer Al_2O_3 type oxide architectures on austenitic 316L stainless steel substrate. The investigation of the coating structure and morphology was carried out by scanning electron microscopy (SEM - EDS) and X-ray diffraction (XRD) measurements. The adhesion test of the obtained coatings was performed using the Test Scrach method.The corrosion behaviour of NiCrAlY and Al_2O_3 multilayer oxide architectures on 316L stainless steel substrate was determined in highly corrosive environment (molten Pb). Corrosion tests were performed in liquid lead at 400 ^{0}C, 450 ^{0}C, and 500 ^{0}C, on 316L stainless steel. Short-term corrosion tests were also performed

on coated and uncoated AISI 316L steel at 550 ^{0}C,. Corrosion tests were carried out in stagnant lead without oxygen control system according to conditions - ICN Pitesti.

Chapter 8 entitled "**Obtaining layered and multilayer oxide architectures of the type ZrO_2Ce - LZO - GZO -TiO_2, Al_2O_3 - LZO - GZO, Al_2O_3, Al_2O_3 -TiO_2, Al_2O_3 - LZO - GZO -TiO2, Al_2O_3 -YSZ - LZO- GZO**" covers obtaining multilayer oxide architectures on austenitic 304L stainless steel substrate by the EB-PVD method. The coatings were realized with and without NiCrAlY, Al_2O_3, using ZrO_2 doped with various rare earth oxides (R- La, Ga, Y) and TiO2. The investigation of the coating structure and morphology was performed by scanning electron microscopy (SEM - EDS) and X-ray diffraction (XRD) measurements. The determination of the adhesion of the obtained coatings was performed using the Test Scrach method, and the electrochemical corrosion studies were carried out at room temperature, in an ASTM corrosion cell with a volume of 1 L. The electrolyte solution used was H_2SO_4 1N, the experiments were carried out after 60 minutes of immersion of the electrodes in the studied electrolyte solution.

Chapter 9 entitled **"Final conclusions, original contributions and future perspectives**" highlights how to obtain multilayer oxide architectures by the EB - PVD cobinatorial method and the resistance of the coatings to the corrosion process in different environments. Thus, oxide layer and multilayer architectures were obtained using NiCrAlY alloy as an adhesion layer. For the oxide coatings, Amperite 740 – Al_2O_3, ZrO_2 doped with rare earth oxides (LZO, GZO,YSZ) obtained by hydrothermal synthesis and TiO2 were used. The substrate used for deposition was 304L and 316L austenitic stainless steel, which was previously cleaned and degreased in isopropyl alcohol and acetone solution by ultrasonication.

The obtained oxide architectures were characterized using X-ray diffraction (XRD) measurements, scanning electron microscopy (SEM - EDS), Test Scrach method. The performances of the coatings were tested by corrosion in different solutions and media: NaCl solution of different concentrations, respectively 0.06M, 0.2M, 0.4M and 0.6M, molten Pb according to ICN-Pitesti conditions and 1N H2SO4 solution. By comparing the oxide coatings obtained by the EB-eam method, the advantages of using layer and multilayer oxide architectures on different austenitic 304L and 316L stainless steel substrates were demonstrated. Thus, dense coatings with low porosity and high improvement in the protection of austenitic stainless steel against corrosion process were obtained.

Following the own results obtained in the PhD thesis and the collaboration of data from the literature in the future it would be of interest to continue research in the development of

new multilayer oxide architectures on other types of thin coatings that can find their applicability in industry for extreme conditions in correlation with strategic areas of development of unconventional energy equipment and systems.

Chapter 1
CURRENT STUDY OF NATIONAL AND INTERNATIONAL RESEARCH ON THIN FILMS IN THE FIELD OF THE PHD TOPIC

1.1 General considerations

The need to increase the life of components by protecting their surfaces from wear and corrosion has accelerated the development of new surface studies in mechanical engineering. Initially, some design changes were made to overcome the above mentioned problem. Nowadays, several techniques are used that allow the modification of surface characteristics such as wear resistance properties by depositing ultra-hard thin films, usually called coatings. The use of coatings improves the behaviour of the surface to abrasion, erosion, adhesion or fatigue, protecting it against corrosion, improves the surface appearance, decreases residual stresses and friction coefficients as well as chemical stability. Because of the importance of these aspects, many researchers have carried out extensive studies in the field of mathematical modelling and numerical simulation of coatings. There are also studies on the thermal conductivity of coatings, since the thermal conductivity of substrates is a characteristic that influences the performance of the mechanical properties of coatings. In these studies, it is very important to consider the correct interpretation of thermal and mechanical analyses. Other studies, such as the improvement of thermal insulation behavior of thermal barrier coatings, vapor behavior from material and gas deposition, plasma enhancement by optimizing the vacuum system or the study of the collision process between target and substrate, have also been performed using Computational Fluid Dynamics (CFD) numerical simulation [1].

Physical vacuum deposition is a well-established coating. that has been vigorously exploited by many industries such as electronics, optics and decorative coatings. In addition, recent advances make new applications in physical vapour deposition possible in other industries. By examining past and present developments in physical vapour deposition, we can make a realistic assessment of its potential for the future [2-3].

Thin film deposition is the process of creating and depositing thin films on a material substrate. These coatings can be made from many different materials. Thin film coatings also have many different characteristics that are used to modify or improve a particular element of the substrate's performance. "Thin" is, of course, a relative coating, but in most cases thin-film deposition techniques are designed to produce coatings only tens of nanometres thick. At present, thin films are commonly thought of in relation to semiconductors. However, thin films are important in a multitude of other areas where layers of micron thickness are needed. Thin films are important because they modify the surface interactions of the substrate with new bulk substrate properties. Thin films have a range of properties and uses depending on the application areas:

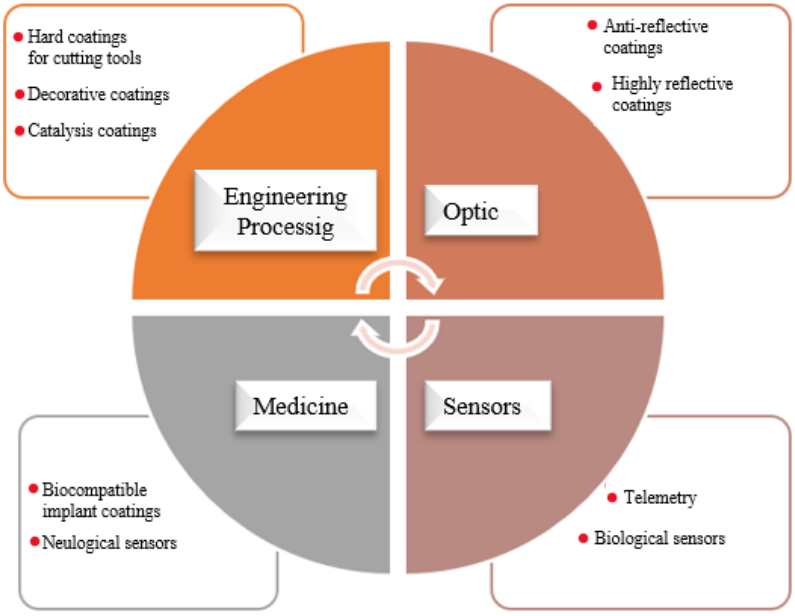

Fig. 1.1. *Areas of use for thin films*

1.2. Classification of thin film deposition processes

Over the years, various materials have been synthesised as thin films because of their potential technological importance and scientific interest in their properties. These have a very wide range of applications and range from nanostructures to the most reliable and cost-effective thin film coatings. Depending on the nature of the deposition process, the techniques used to make thin films (thin film deposition), can be classified into two groups, namely, physical and chemical deposition processes [10].

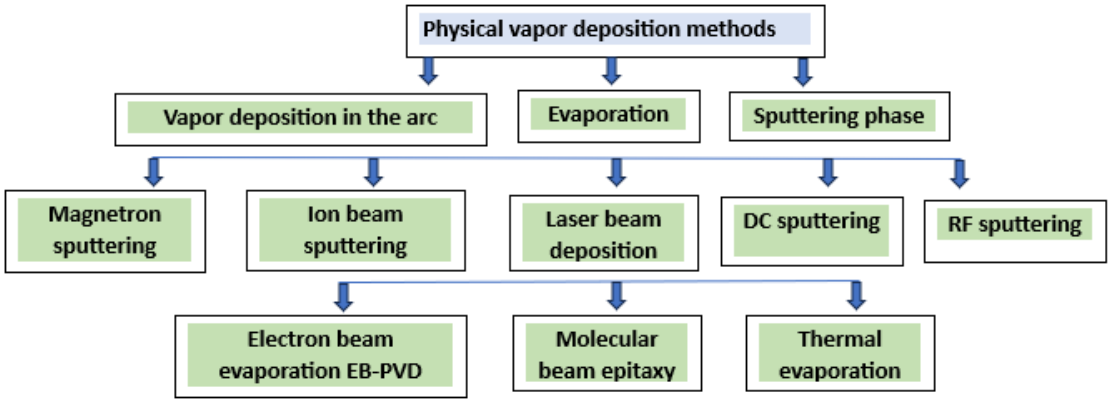

Fig. 1.2. *Thin film deposition (PVD) techniques [10].*

1.3. Physical vapour deposition (PVD) method

PVD means physical vapour deposition. PVD coating refers to a variety of thin-film deposition techniques in which a solid layer, a solid material, is vaporised in a vacuum medium and deposited on substrates as a coating layer of pure material or alloy composition. This evaporates or sputters a material, producing a gaseous column or beam that deposits a film on the substrate. Coatings created in this way are very durable and resistant to scratches and corrosion. PVD is useful in the production of devices ranging from solar cells to glasses and semiconductors [11].

Chapter 2

MECHANISMS AND FORMS OF CORROSION IN STEELS

2.1. General notions on mechanisms and forms of corrosion in steels

Corrosion is a natural process, which is defined as the degradation or deterioration of a substance and/or its properties, usually a metal, over a period of time due to exposure to the environment [57]. It is an exergonic process because the metal tends to the lowest possible energy state. Therefore, metals such as aluminium and steel have a natural tendency to return to their lowest energy state when they combine with oxygen and water to form hydrated oxides of aluminium and iron (corrosion products). These corrosion products are the final state of processed metals that degrade over time when exposed to weathering. Thus, the life cycle from mining ores and processed, to industrial products and finally back to the natural state.

The environment to which metals are exposed consists of the entire environment in contact with the metal. The main factors used to describe the environment are

- the physical state of the environment, whether gaseous, liquid or solid;

- chemical composition, which includes constituents and concentrations;

- temperature.

2.2. Identification of different forms of corrosion

The different forms of corrosion are corrosion phenomena classified according to their appearance. The three categories are:

- Group 1: easy to identify by ordinary visual examination;

- Group 2: may require additional means of examination;

- Group 3: verification is usually required by microscopy (optical, electron microscopy, etc.).

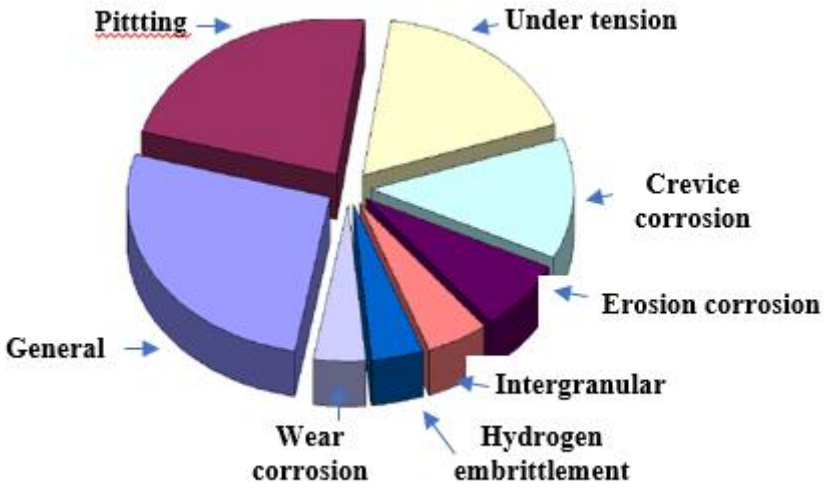

Fig. 2.2. *Statistica distributiei a diferitelor tipuri de coroziune pe plan Mondial [65].*

2.4. Types of corrosion

Corrosion damage can occur in several ways, e.g., cracking failure, loss of strength, etc. Forms of corrosion are: uniform attack, galvanic corrosion, erosion corrosion, stress corrosion, crevice corrosion, erosion corrosion and intergranular corrosion [68, 69].

2.4.1. Uniform corrosion

Uniform corrosion is the attack of a metal at essentially the same rate in all exposed areas of its surface (Fig.1). At no point is the penetration of the metal by corrosion twice the average rate. Rusting of steel in the atmosphere and corrosion of copper alloys in seawater are common examples where uniform corrosion is usually encountered. Steel immersed in seawater also undergoes uniform corrosion, but may also undergo non-uniform attack under certain circumstances [68].

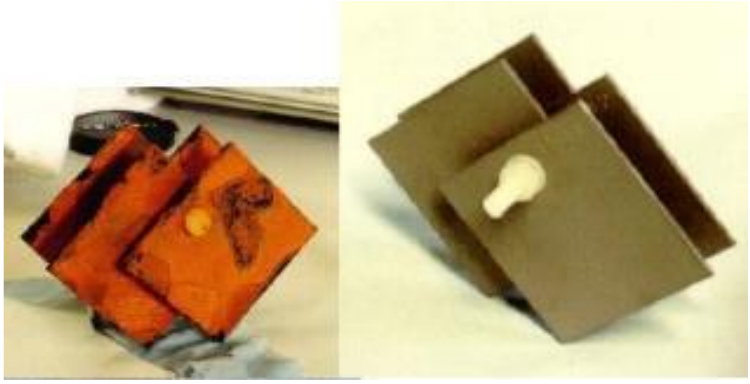

Fig. 2.3. *Uniform metal attack [68].*

2.6. Corrosion protection with steel coatings

Corrosion protection is probably the largest application area for coatings, both in terms of total areas covered and volume of business. The real costs of corrosion damage are estimated at around 3-4% of a country's gross domestic product (GDP) per year. [81].

The two-year global study, released at the CORROSION 2016 conference in Vancouver, B.C., examined the economics of corrosion and the role of corrosion management in establishing industry best practices.

The annual cost of corrosion globally, according to the study by NACE International, is $2.5 trillion (approximately 3.4% of global GDP). The study found that implementing corrosion prevention best practices could result in global savings of 15-35% of this cost ($375-$875 billion). Corrosion prevention would improve the service life and durability of structures, significantly avoiding premature destruction of the structure and losses associated with periodic inspections. [82]

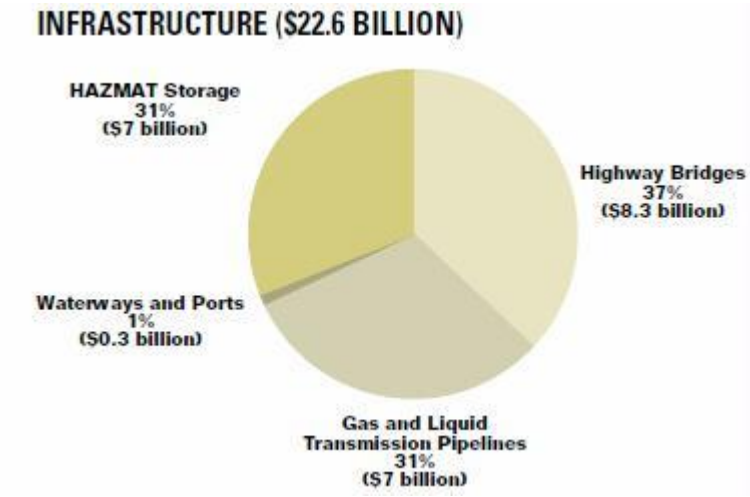

Fig. 2.11. *Cost of corrosion infrastructure [82].*

Chapter 3
RESEARCH OBJECTIVES AND METHODOLOGY

3.1. Objectives of the PhD thesis

The main objective of the thesis is to select the development and realization of Al_2O_3, ZrO_2 and TiO_2 based oxide layer and multilayer architectures, obtained by the EB-PVD combinatorial process, capable of responding to thermo-chemical corrosion stresses, with potential applications in the development of new components for thermal equipment operating under extreme environmental conditions. Advanced multi-layer nanostructured material solutions will thus be designed to provide partial or total replacement of super-refractory alloys with high content of critical materials (Cr, Ni, Mo) currently used in such applications.

In order to achieve the main objective of the PhD thesis, the following scientific and technical objectives have been considered:

- Specific selection of the required materials used as substrate-support on which Al_2O_3, ZrO2 and TiO_2 based oxide layer and multilayer architectures will be deposited by the EB-PVD combinatorial method;
- Design of Al_2O_3, ZrO_2 and TiO_2 based layered and multilayered oxide materials and architectures for extreme temperature and corrosion conditions by predictive

thermodynamic calculations using specialized software and literature data; (HSC v.9-Outokumpu Finland, MATCALC-access on line to ENEA Rome network) and recent electronic database (NIST Phase Diagrams 2016-multiple license purchased from American Ceramic Society).

- Obtaining multilayer oxide architectures such as Al_2O_3; Y_2O_3 - doped ZrO_2; Ce_2O_3 - doped ZrO_2; $La_2Zr_2O_7$ on 316L austenitic stainless steel substrate by combinatorial EB-PVD method and demonstrating the proposed concept by corrosion testing of oxide architectures obtained in NaCl electrolyte solution of different concentrations, i.e. 0.06M, 0.2M, 0.4M and 0.6M, according to ASTM G61-86 standard (Reapproved 2003);

- Obtaining multilayer oxide architectures such as Al_2O_3, ZrO_2 doped with rare earth oxides (CeO_2; Nd_2O_3; La_2O_3; GdO_3), on austenitic 304L stainless steel substrate by combinatorial EB-PVD method and corrosion testing of oxide architectures obtained in 1N H_2SO_4 solution.

- Obtaining experimental models of Al_2O_3 layer oxide architectures samples on 316L austenitic stainless steel substrate by the EB-PVD combinatorial method and demonstrating the proposed concept by performing corrosion tests in molten lead at ICN Pitesti.

- Obtaining of layered and multilayer oxide architectures such as: layer of needles (NiCrAlY) - LZO - GZO -TiO_2, Al_2O_3- LZO - GZO, Al2O3, Al_2O_3-TiO_2, Al_2O_3 - LZO - GZO-TiO_2, Al_2O_3-YSZ - LZO- GZO on 304L austenitic stainless steel substrate by combinatorial EB-PVD method and corrosion testing of the obtained oxide architectures in 1N H $_2SO_4$ solution.

Chapter 4

THERMODYNAMIC MODELING, OBTAINING AND CHARACTERIZATION OF DOPED ZrO2 NANOSTRUCTURED POWDER

4.1. Thermodynamic modeling of the hydrothermal synthesis processes of ZrO_2 doped with Y_2O_3

Three polymorphic forms, namely monoclinic (m), tetragonal (t) and cubic (c), can be accepted for pure zirconium dioxide, which can be obtained by temperature and composition ranges at steady state for pure zirconium. At temperatures below 1100 °C, pure ZrO_2 has a monoclinic (m) structure. By heating between 1100 °C and 2370 °C, the monoclinic form transforms into a tetragonal phase, and at temperatures between 2370 °C and 2706 °C it exists as a cubic phase. The two tetragonal and cubic phases can be stabilised at low temperatures by introducing additives.

To date, several techniques have been developed for the preparation of doped ZrO_2 such as sol-gel method, co-precipitation, colloidal synthesis and hydrothermal method. Studies have shown that 3%Y-doped zirconium has excellent thermal barrier, anti-corrosion and wear resistance properties. [124].

The formation of ZrO_2 under hydrothermal conditions occurs by stepwise hydrolysis of ionic species through valence reduction:

Zr4+ > Zr(OH)3+ > Zr(OH)22+ > Zr(OH)3+ > Zr(OH)4.

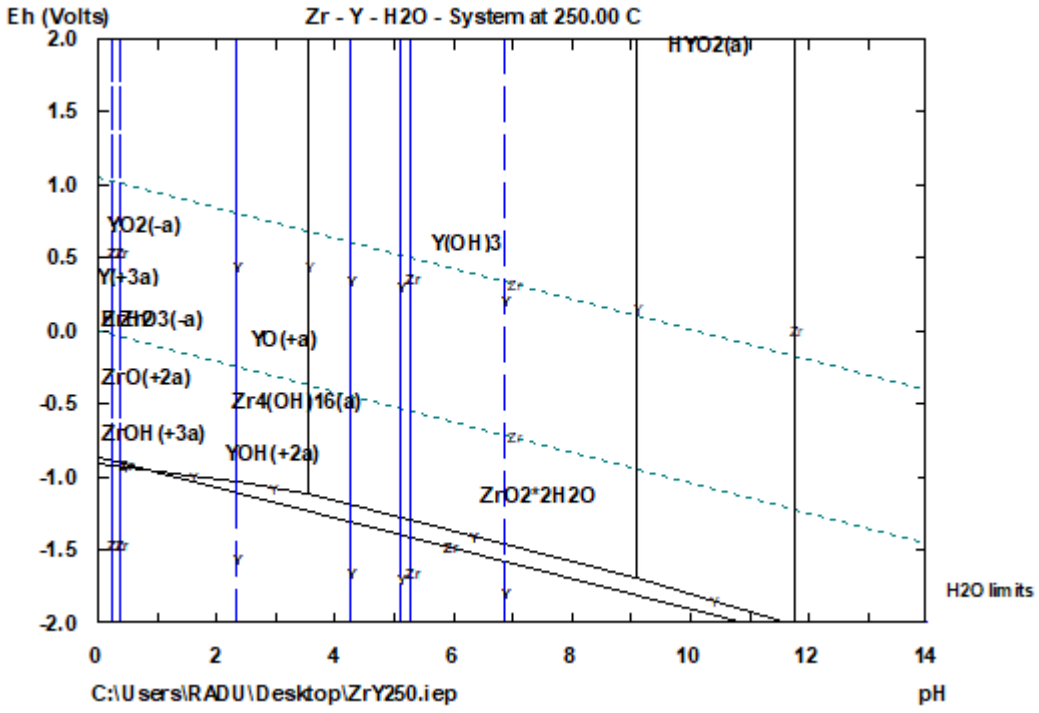

Fig. 4.2. *Pourbaix diagram for the Zr-Y-O-H system at 250 ^{0}C.*

4.2. Thermodynamic modelling of hydrothermal synthesis processes of $La_2Zr_2O_7$

Figures 4.3. and 4.4. show the Pourbaix diagram of the La-O-H system at room temperature and under hydrothermal conditions at 250 ^{0}C.

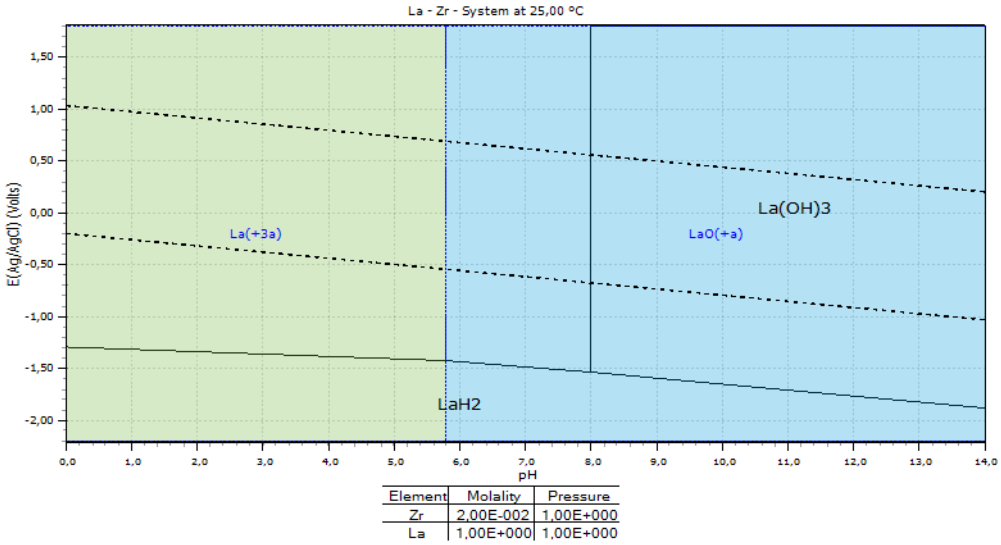

Fig. 4.3. Pourbaix diagram for the La-O-H system at 25 ^{0}C.

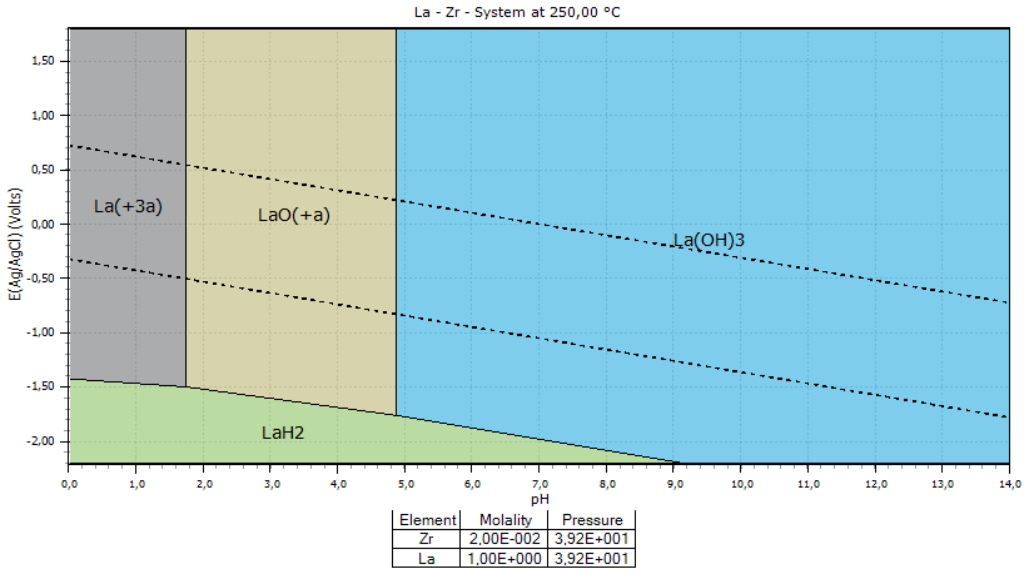

Fig. 4.4. Pourbaix diagram for the La-O-H system at 250 ^{0}C.

Increasing the solution temperature leads to increasing the stability of the solid species La(OH)3 over a wider pH range. At room temperature solid species formation occurs in the pH range = 8÷14 and under hydrothermal conditions solid species formation in the pH range = 5÷14.

4.4. Physico-chemical and structural characterization of doped ZrO_2 powder obtained by hydrothermal synthesis

For the characterization of oxide powders obtained by hydrothermal synthesis at INCDMNR-IMNR, a complex methodology has been established to determine the chemical and structural composition, by applying various methods of analysis: ICP-OES, DSC-TG, XRD, SEM-EDX.

Quantitative chemical analysis by inductively coupled plasma optical emission spectrometry (ICP-OES) method according to ASTM E 1479-16 standard was carried out on an equipment type Agilent 725-Agilent Technology USA, on the powders for oxide materials obtained, the elements: Zr; La; Y; Ce were determined. The results of this analysis are presented in Table 4.

Table 4.1. *Quantitative chemical analysis on powder samples of the tested oxide materials $ZrO28\%MY_2O_3$, $ZrO_28\%MCe_2O_3$, $La_2Zr_2O_7$.*

Sample code	***Sample name***	***UM %***			
		Zr	***La***	***Y***	***Ce***
LZ - PN1	Powder ZrO_2 + La	21,32	31,44	-	-
ZrO_2 - 8Y	Powder ZrO_2 + Y	49,36	-	8,32	-
ZrO_2 – 8 Ce	Powder ZrO_2 + Ce	48	-	-	8,21

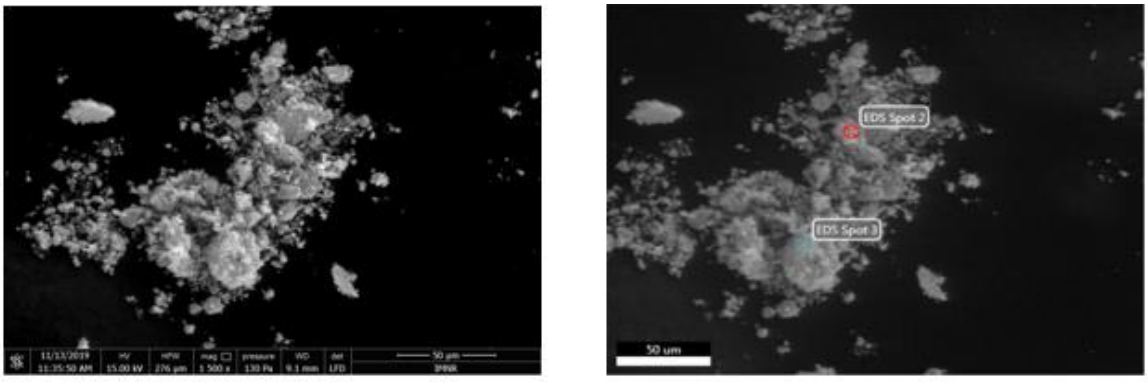

Fig. 4.14. *SEM image at 1500 X for LZ oxide material and EDS point selection*

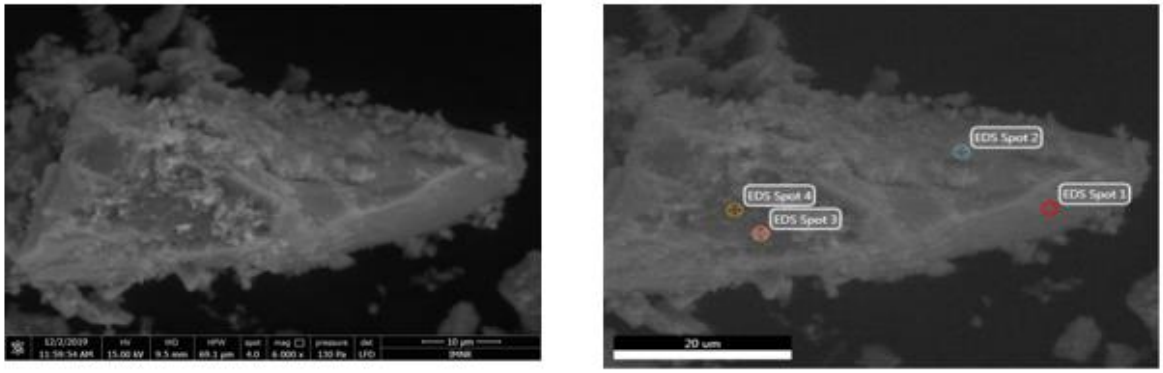

Fig. 4.16. *SEM image at 6000 X for ZrO2 - 8Y oxide material and EDS point selection*

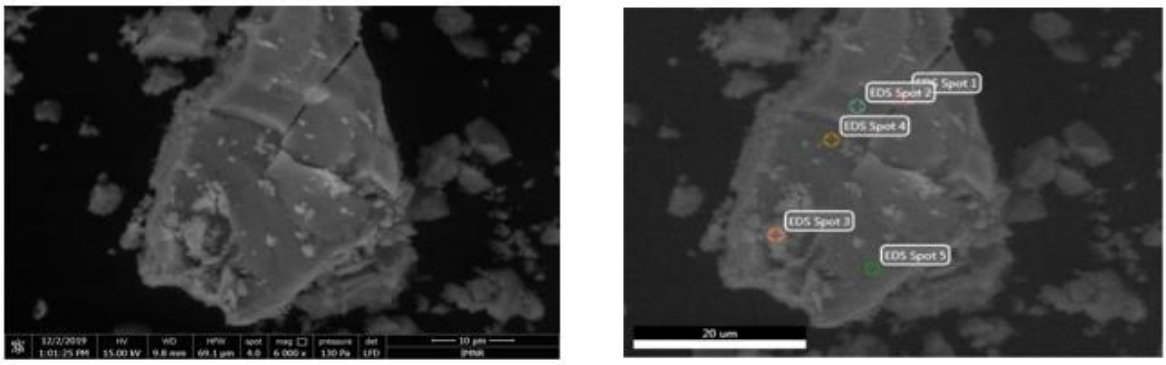

Fig. 4.18. *SEM image at 1500 X for ZrO2 - 8Ce oxide material and EDS point selection*

Chapter 5

OBTAINING AND CHARACTERIZING MULTILAYER OXIDE ARCHITECTURES OF THE TYPE Al2O3; ZrO2 DOPED WITH Y2O3; Ce_2O_3; La 2ZrO OBTAINED BY THE COMBINATORIAL EB-PVD METHOD

5.1. Obtaining multilayer oxide architectures Al_2O_3; ZrO_2 doped with Y_2O_3; Ce_2O_3; $La_2Zr_2O_7$, on 316 L stainless steel substrate by EB-PVD method

In order to obtain multilayer oxide architectures such as Al_2O_3; ZrO_2 doped with Y_2O_3; Ce_2O_3; LaZr2O, 316L stainless steel plates with dimensions of 30x50x2 mm were used as substrate, which were previously cleaned and degreased in an isopropyl alcohol/acetone bath, using ultrasound at the same time (Figure 3.9.) [127-131].

The substrates thus cleaned, were subsequently fixed in a device that is coupled to a rotating mechanism, which rotates at 20 rpm during the coating process, heating the parts

(substrates) with a parabolic surface heater to a temperature of ca. 400o C in a vacuum of approx. 10^{-7} Torr.

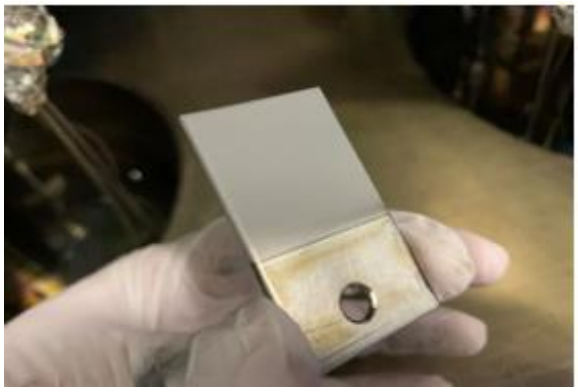

Fig. 5.3. *EB-PVD deposition sample of acrosium (NiCrAlY) and Al_2O_3*

5.2. Characterization of the obtained multilayer oxide architectures: EB - PVD deposition samples of acrosium (NiCrAlY) and Al2O3 and ZrO_2 doped Y_2O_3; $La_2Zr_2O_7$; surface layer: ZrO_2 doped with Ce_2O_3 on 316 L stainless steel substrate by EB - PVD method

In order to characterize the experimental patterns of multilayer oxide deposition on 316L stainless steel substrate obtained by EB-PVD, the samples were labelled and then a complex investigation methodology was established by applying different analysis methods: SEM-EDX, X-ray diffraction test, scrach test.

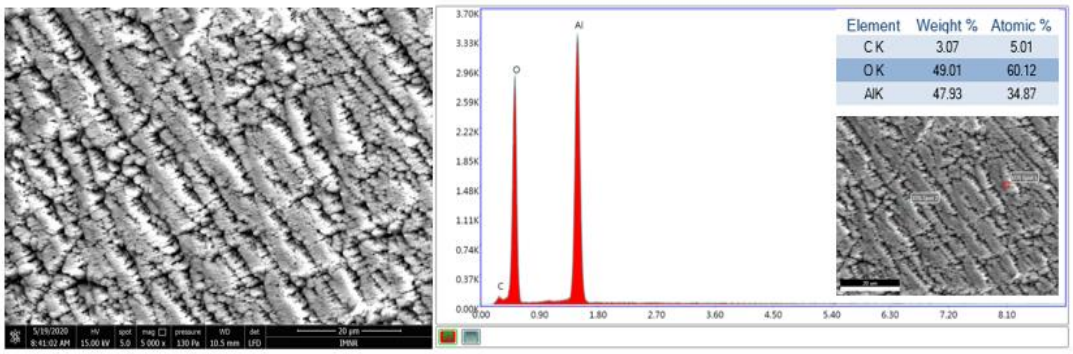

Fig. 5.5. *EDS spectrum for the sample obtained by the EB- PVD- acros (NiCrAlY) and Al_2O_3 process*

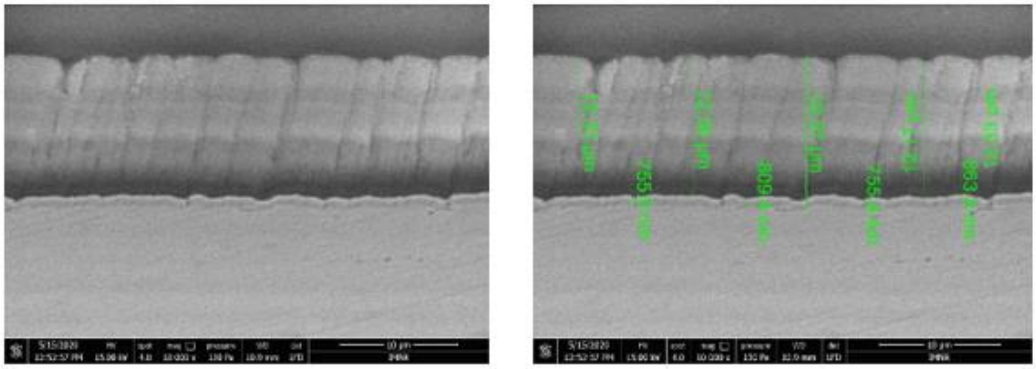

Fig. 5.6. *SEM cross-sectional image at 10. 000 X for acrosium (NiCrAlY) and Al_2O_3 oxide material*

SEM and EDS surface microstructural appearance of deposition samples: acros layer and oxide multilayers Al_2O_3 and ZrO_2 doped Y_2O_3; $La_2Zr_2O_7$; surface layer: ZrO_2 doped with Ce_2O_3 on 316L stainless steel substrate obtained by EB-PVD process can be seen in Figure 5.8.

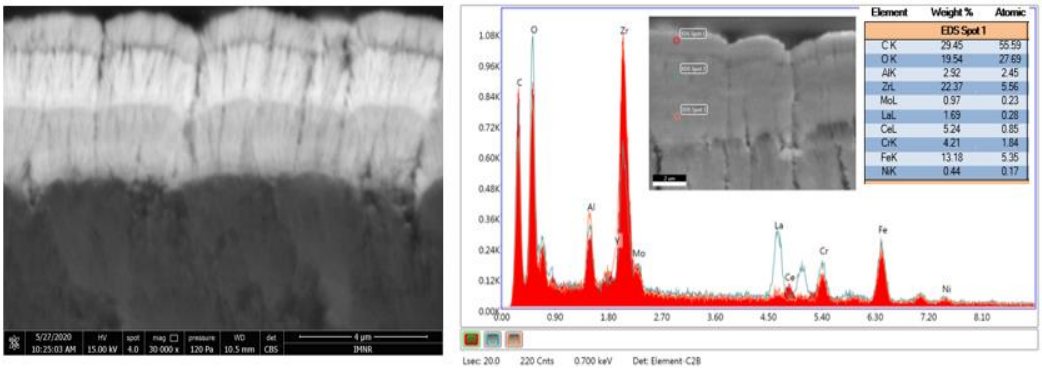

Fig. 5.8. EDS spectrum for the sample obtained by the EB- PVD- acros (NiCrAlY) and Al_2O_3 and ZrO_2 doped Y_2O_3; $La_2Zr_2O_7$; surface layer: ZrO_2 doped with Ce_2O_3.

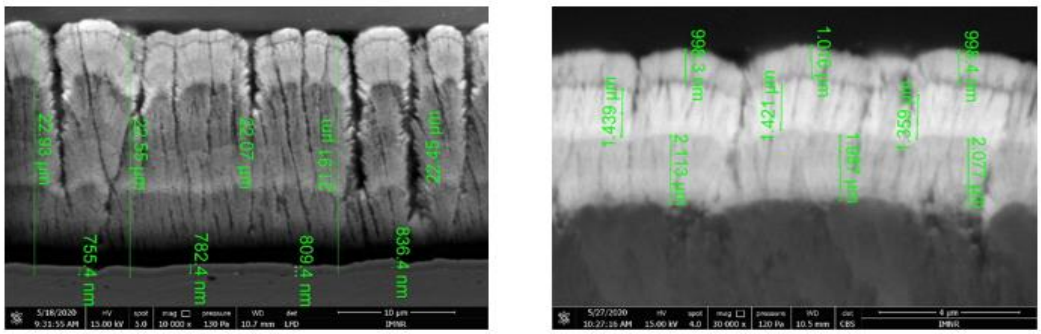

Fig. 5.9 *SEM cross-sectional image at 10.000 X magnifications for acrosstalk oxide material (NiCrAlY) and Al_2O_3 and ZrO_2 doped Y_2O_3; $La_2Zr_2O_7$; surface layer: ZrO_2 doped with Ce_2O_3 on 316L stainless steel substrate.*

Scanning electron microscopy images indicate the morphological and structural appearance of the samples studied. It can be observed the growth size on 316L stainless steel substrate of columnar gratings of oxide compounds such as: Al_2O_3 and ZrO_2 doped Y_2O_3; ; $La_2Zr_2O_7$; surface layer: ZrO_2 doped with Ce_2O_3, resulting from thermal evaporation process with E-beam. The microscopic heterogeneous aspect of the material structure resulting from the deposition is also shown. As shown in Figure 5.6., the shape of the deposited layer is highlighted as well as the diameter ranging from 755.4 - 863.3 nm having the acrose layer and the Al_2O_3 layer having a thickness of about 12 μm. The EDS spectra of the sample obtained by the EB- PVD- Acrochrome (NiCrAlY) and Al_2O_3 process confirmed the presence of these elements.

Chapter 6

OBTAINING AND CHARACTERISING MULTISTRATE OXIDE ARCHITECTURES OF TYPE: NiCrAlY - ZrO_2 DOPED WITH CeO_2 and Al_2O_3 BY COMBINATORIAL EB-PVD METHOD

6.1. Obtaining multilayer NiCrAlY- ZrO_2 multilayer oxide architectures doped with CeO_2 and Al_2O_3 on 304 L stainless steel substrate by EB-PVD method

Analysing the results obtained from the preliminary experiments carried out in Chapter 5 of this PhD thesis, three changes have been established for this chapter, which will be carried out in the structure of the submission of these materials, namely:

- the use of austenitic 304L stainless steel as substrate;

- the intercalation of an intermediate layer between the NiCrAlY steel layer and the CeO_2 - doped ZrO_2 surface layer;

- Al_2O_3 (Amperit 740) surface layer.

In order to obtain multilayer oxide architectures of the type NiCrAlY- ZrO_2 doped CeO_2 - Al_2O_3; ZrO_2 doped, 304L stainless steel plates of the following dimensions were used: 30x50x2 mm, respectively 55x55x2 mm, which were previously cleaned and degreased in an isopropyl alcohol/acetone bath, using ultrasound at the same time.

The cleaned substrates were then fixed in a device that was coupled to a rotating mechanism.

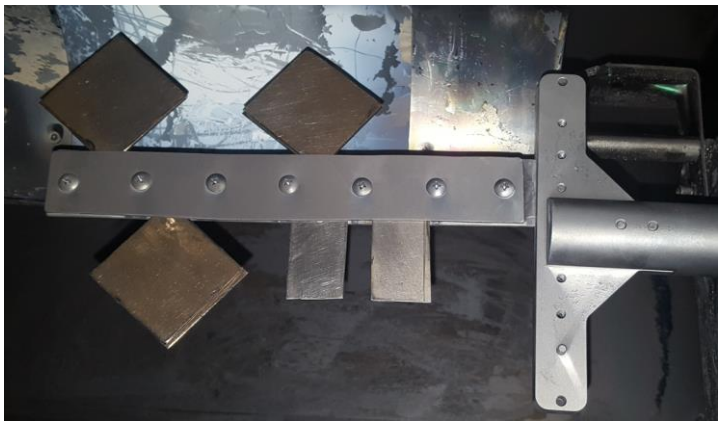

Fig. 6.1. *304L stainless steel substrates cleaned and fixed to the device..*

After completion of the E-beam deposition experiments, the samples were unloaded from the multiple electron flow deposition facility Fig.3.1. and subsequently marked in preparation for analysis. Figures 6.1 and 6.2. show aspects at the completion of these EB-PVD deposition experiments.

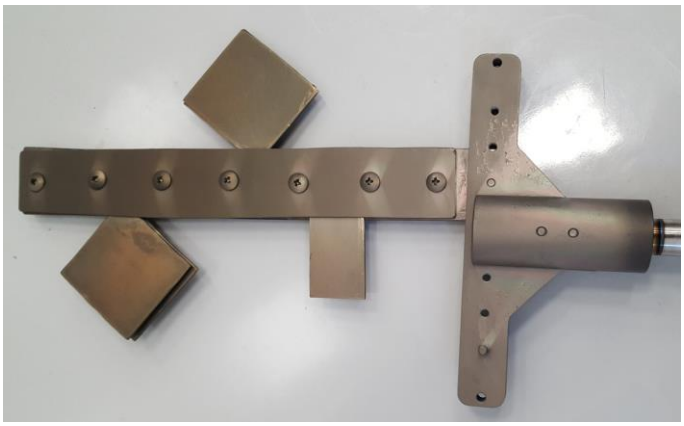

Fig. 6.3. *EB - PVD deposition samples of acrosium (NiCrAlY) and CeO_2 -doped ZrO_2*

Fig. 6.4 *EB- PVD deposition samples of (NiCrAlY)- ZrO_2 doped with CeO_2 -Al $_2O_3$*

6.3. Electrochemical corrosion resistance testing of multi-layered oxide architectures of NiCrAlY – ZrO_2 doped with CeO_2 and Al_2O_3 on 304 L stainless steel substrate obtained by EB-PVD method

Electrochemical corrosion studies were carried out at room temperature in a flat corrosion cell (Figure 3.5), equipped with 3 electrodes: working electrode - material to be analysed, exposed surface 16.9 cm2; reference electrode - Ag/AgCl in 3M KCl solution; counter electrode - 316 stainless steel. The 3 electrodes are coupled to a PGSTAT 128N Autolab potentiostat/galvanostat (Methrom) connected to a computer with NOVA 2.1 software. The electrolyte solution used was 1N H2SO4, according to ASTM G5-14 standard. [129]. The experiments were carried out after 60 minutes of immersion of the electrodes in the electrolyte solution studied.

In this chapter of the PhD thesis the corrosion resistance of the following types of coatings on 304L stainless steel substrate was studied for the following samples:

- P_0 (304L stainless steel (uncoated);

- P_1 stainless steel 304L- NiCrAlY- ZrO_2 doped with CeO_2;

- P_5 stainless steel 304L- NiCrAlY - ZrO_2 doped with CeO_2 - Al_2O_3;

- P_2 stainless steel 304L- NiCrAlY- ZrO_2 doped with CeO_2;

- P_6 stainless steel 304L- NiCrAlY -ZrO_2 doped with CeO_2 - Al_2O_3.

Figures 6.22 - 6.23. show the Tafel curves in 1N H_2SO_4 electrolyte solution.

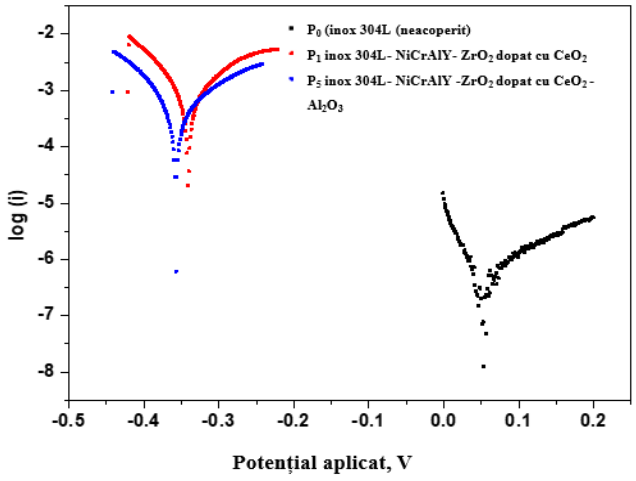

Fig. 6.22. *Tafel curve in 1N H_2SO_4 electrolyte solution for samples P_0, P_1, P_5.*

6.4. Surface morphology characterization of samples P_0 (stainless steel 304L (uncoated), P_1 and P_5 after corrosion in 1N H2SO4 solution by SEM method

In order to highlight the morpho-structural aspect of the samples after the corrosion process in 1N H_2SO_4 solution, samples P_0 (304L stainless steel (uncoated) and one sample with different coatings from the other samples were investigated, namely sample P_1 304L stainless steel - NiCrAlY - ZrO_2 doped with CeO_2 and sample P_5 304L stainless steel - NiCrAlY – ZrO_2 doped with CeO_2 - Al_2O_3. Microstructural investigation of the samples was performed by scanning electron microscopy (SEM), type FEI Qanta 250, Fig. 3.17. present in the analytical laboratory of IMNR.

Figure 6.17. shows the SEM micrograph of sample P0 - uncoated stainless steel taken on the surface and in section:

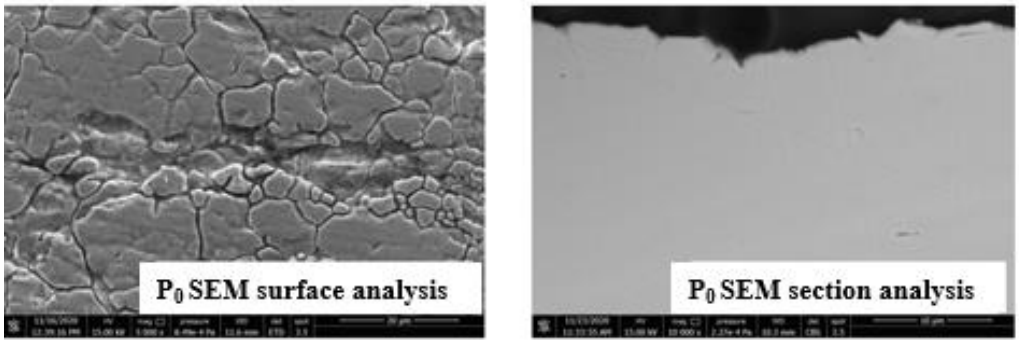

Fig. 6.17. *SEM images at surface and cross-sectional re-sampled sizes (M= 5000 X ,10.000X) for sample P_0 - uncoated stainless steel*

Figure 6.18. shows the SEM micrograph of sample P_1 - 304L stainless steel coated with NiCrAlY- ZrO_2 steel doped with CeO_2 on the surface and in section:

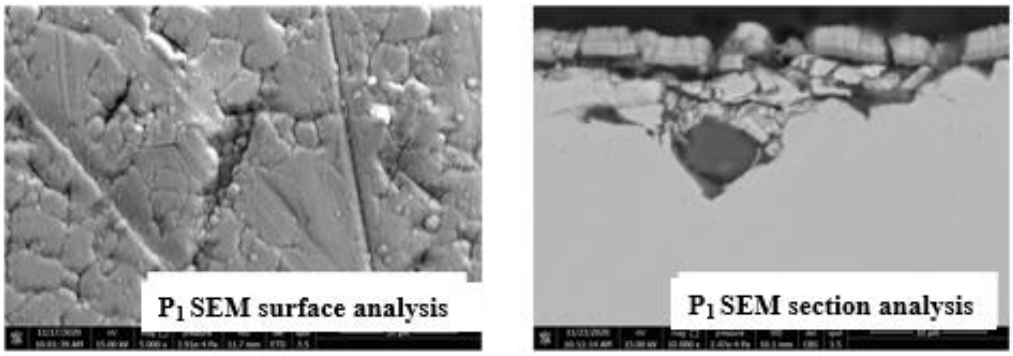

Fig. 6.18. *SEM images at surface and cross-sectional re-samples (M= 5000 X ,10.000 X) for sample P_1- 304L stainless steel coated with NiCrAlY- ZrO_2 doped with CeO_2*

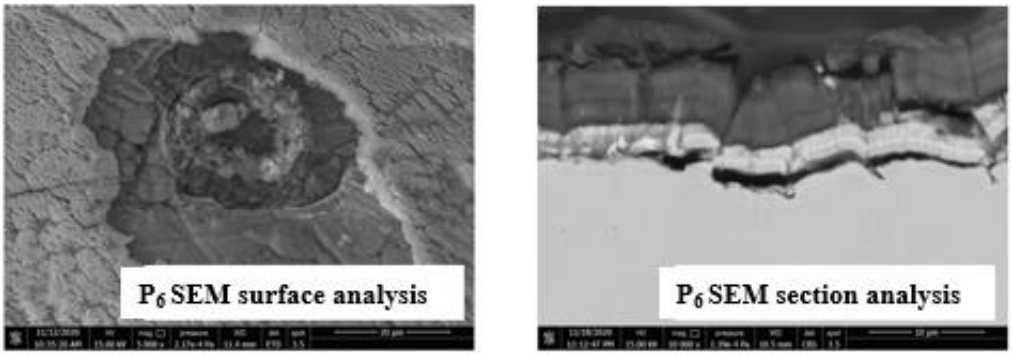

***Fig. 6.19**. SEM images at surface and cross-sectional re-scaled (M= 5000 X ,10.000 X) for sample P1- 304L stainless steel coated with NiCrAlY- ZrO_2 doped with CeO_2 - Al_2O_3*

It is observed that samples P1 and P5 characterized by scanning electron microscopy are morphologically similar. After the corrosion process, it is observed that in the case of sample P2 (304L stainless steel coated ZrO_2 doped with CeO_2) the sulphuric acid attacks the sample in section, the sample is corroded up to the steel layer, while in the case of sample P_5 (304L stainless steel - ZrO_2 doped with CeO_2 - Al_2O_3), it corrodes more at the surface, not being attacked by sulphuric acid up to the stainless steel substrate. Moreover, it can be seen from Tables 6.2 and 6.3. that the corrosion rates are comparable in order of magnitude for samples P_1, P_2 (stainless steel with zirconia) and P_5, P_6 (stainless steel with zirconia and alumina). V=16.7 mm/year for P_1 and 8.6 mm/year for P_5, respectively V=15.8 mm/year for P_2 and 11.1 mm/year for P_6.

Chapter 7

OBTAINING AND CHARACTERISING EXPERIMENTAL Al_2O_3 TYPE MODELS ON AUSTENITIC 316L STAINLESS STEEL SUBSTRATE BY THE EB-PVD METHOD FOR FUSED LEAD CORROSION

7.1. Obtaining experimental models of NiCrAlY and Al_2O_3 multilayer oxide architectures on 316 L stainless steel substrate by EB-PVD method

For the experimental corrosion patterns in molten Pb obtained by the combinatorial EB-PVD deposition method, the substrate used in the experiments was austenitic 316L stainless steel in the form of 25x12x3 mm pads, which were previously cleaned and degreased in isopropyl alcohol/acetone using a thermostated ultrasonic bath (Fig. 3.9.).

The substrate plates thus cleaned were then fixed in a device, coupled to the rotating mechanism of the E-beam installation, which rotates at 20 rpm during the coating process. Fig. 7.1.

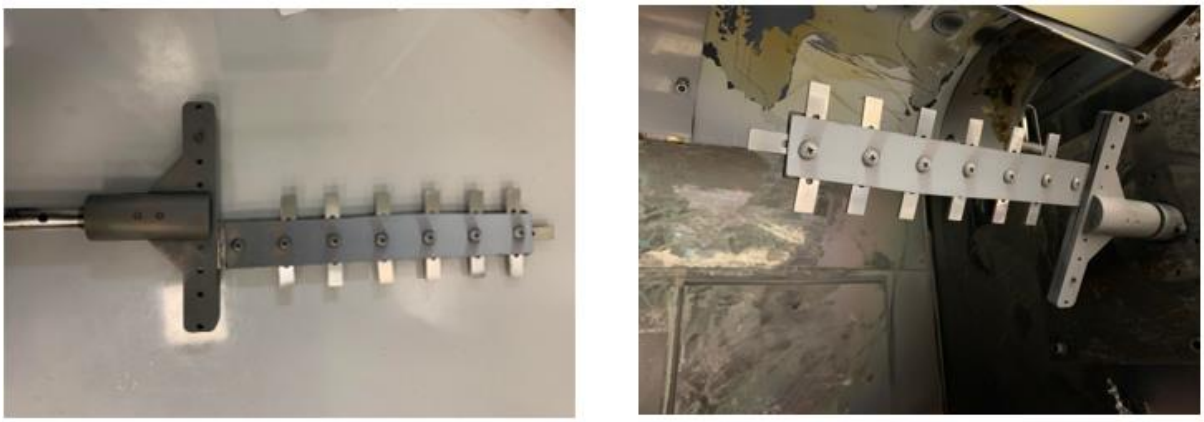

Fig. 7.1. *Attaching the substrate pads to the device and coupling the device to the turning mechanism*

After completion of the E-beam deposition experiments, the samples mounted in the device were discharged from the TORR multiple electron flow deposition facility, Model No: 5X300EB-45KW fig. 3.1. and subsequently marked in preparation for analysis. Figure 7.4. shows aspects at the completion of these EB-PVD deposition experiments, on austenitic 316L stainless steel substrate, oxide multilayers of the type: NiCrAlY and Al_2O_3.

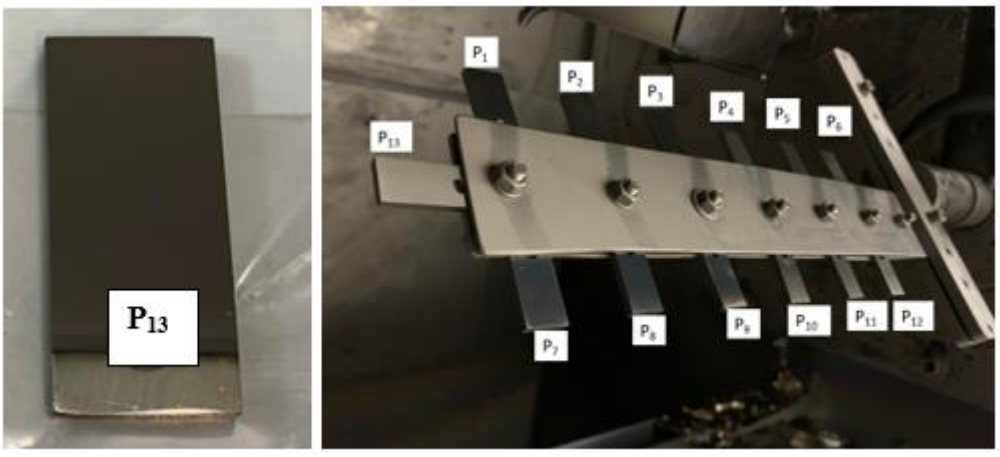

Fig.7.5. *Experimental models of NiCrAl Y and Al_2O_3 oxide architectures on austenitic 316L stainless steel for corrosion in molten Pb*

7.2. Characterisation of multilayer oxide architectures obtained before corrosion testing in liquid Pb

Experimental models of sample deposition of NiCrAlY and Al_2O_3 films(layers) by EB-PVD on a 316L - austenitic stainless steel substrate (25x12x3 mm) were performed. For the characterization of experimental multilayer oxide deposition patterns on 316L stainless steel substrate obtained by EB-PVD, a complex investigation methodology was established on sample P13 at INCDMNR-IMNR, by applying various methods of analysis: SEM-EDS, scrach test, X-ray diffraction.

The morphological appearance corresponding to sample P13 developed on 316L stainless steel support surface using EB-PVD process are shown in Figure 7.6.

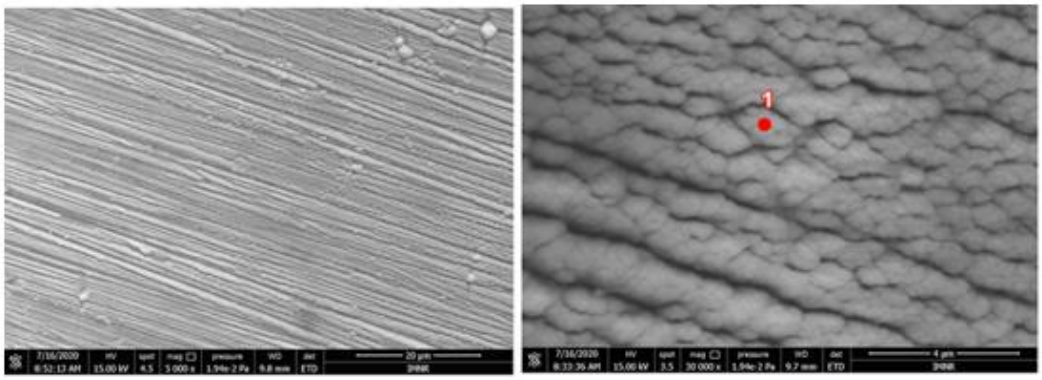

Fig.7.6. *SEM images at different magnifications (M=5,000 X, 30,000 X) re-sampled on the surface for the acrO2 (NiCrAlY) and Al2O3 oxide material of sample P13 and the point selected for EDS analysis*

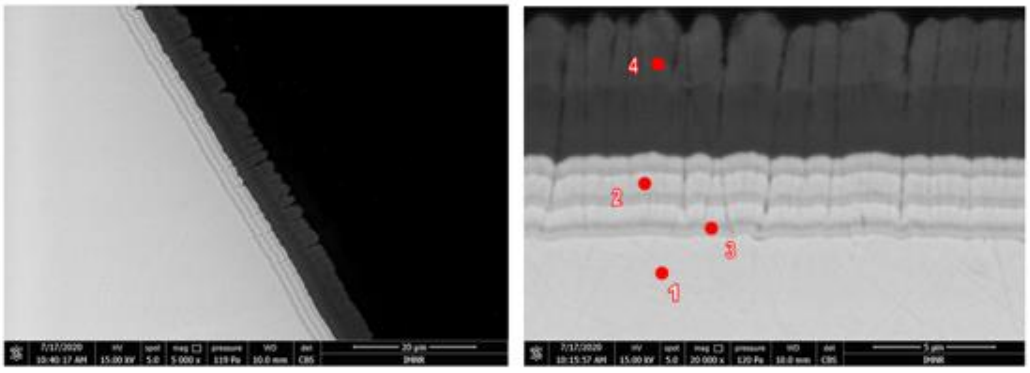

Fig. 7.8. *SEM images at different magnifications (M=5,000 X, 20,000 X) re-sectioned for the acrosstalk (NiCrAlY) and Al_2O_3 oxide material of sample P13 and selected points for*

Tabel 7.2. *Chemical composition of the sample: NiCrAlY - $Al2_2O_3$ on 316L stainless steel according to EDS point analysis*

Punct analizat		Chemical composition, % gr.						
	O	Si	Fe	Cr	Ni	C	Y	Al
EDS Spot 1	1.2	0,38	69,34	20,45	7,46	-	-	-
EDS Spot 2	6,05	-	39,87	8,28	36,18	1.04	1,27	4,78
EDS Spot 3	-	-	45,5	26,80	27,3	-	-	2,77
EDS Spot 4	44							58

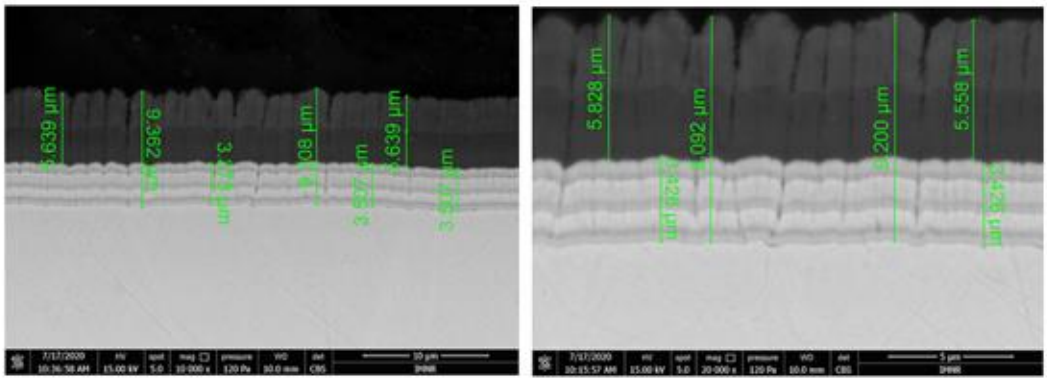

Fig.7.13. *SEM images at different magnifications (M=10,000 X, 20,000 X) with measurements of the cross-sectionally re-sectioned deposited layers for the acros (NiCrAlY) and Al_2O_3 oxide material of sample P13 and selected points*

Sample P13 NiCrAlY- on 316L stainless steel substrate obtained by EB-PVD process, were evaluated by performing a scratch test. The test was carried out with a "Scratch Test NANOVEA"- identor for scratching/adhesion: M0-M1250 conical 120 degree 50 micrometers. The results are shown in Fig. 7.15.

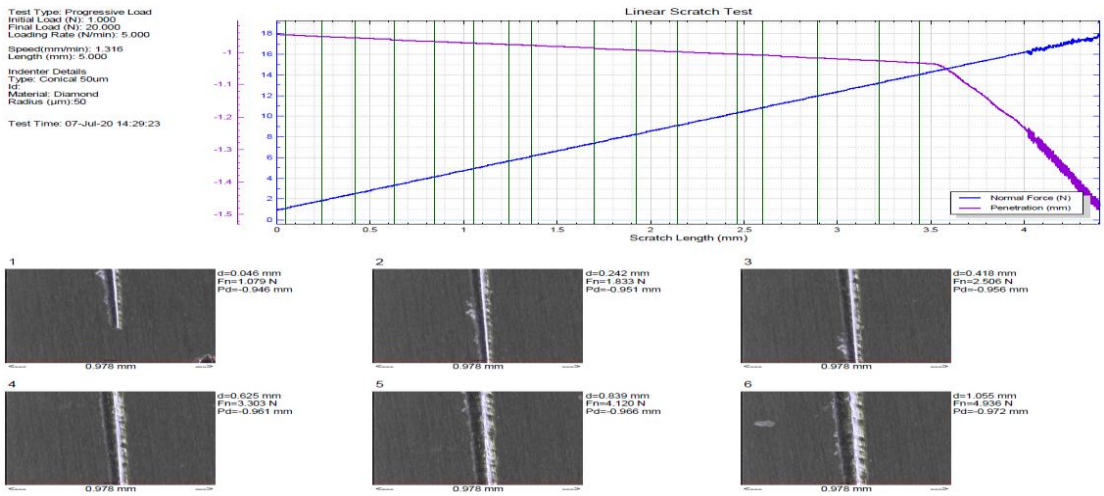

Fig. 7.15. *Adhesion test on P13 NiCrAlY and Al_2O_3 steel specimen on 316L stainless steel substrate obtained by EB-PVD*

7.3. Characterization of oxide architectures for molten lead corrosion testing at ICN Pitesti

Corrosion behaviour of NiCrAlY and Al_2O_3 multilayer oxide architectures on 316L stainless steel substrate was determined in highly corrosive environment (molten Pb). The experimental facility with which the tests were carried out in liquid lead ISTRON - ICN Pitesti (fig.3.6.), for which additional facilities have been developed to allow testing in molten lead environment.

The corrosion test was carried out for 500 h and 1000 h at 550°C. Immediately after removal of the samples from the melt, the surface of the tested samples remains in some areas covered with solidified lead (Figures 7.13 - 7.14). From the visual appearance, it can be seen that the bare samples are covered with a large amount of solidified lead compared to the coated samples.

Fig. 7.13. *Samples tested in liquid Pb at 550°C for 500 h*

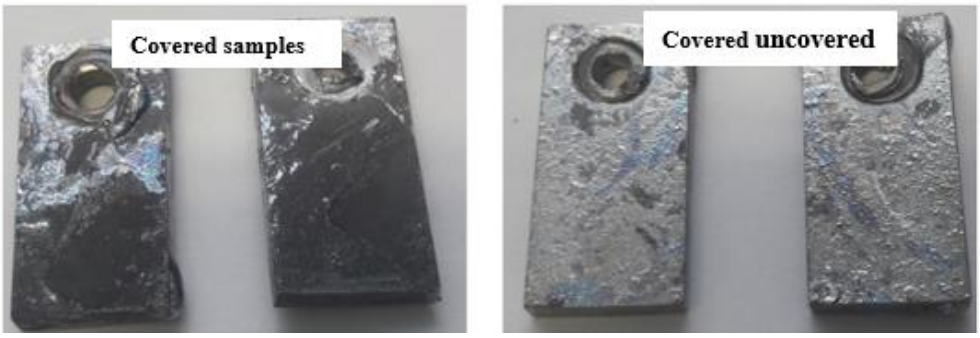

Fig. 7.14. *Samples tested in liquid Pb at 550°C for 1000 h*

An Olympus GX71 microscope was used to analyse the surface of the samples, the thickness of the oxide layer formed or the integrity of the coating after exposure. For this

reason, some specimens were cut in cross-section. The images in Figure 7.15. show that lead did not penetrate the steel substrate and that the structural integrity of the material is not affected after 500 hours of exposure.

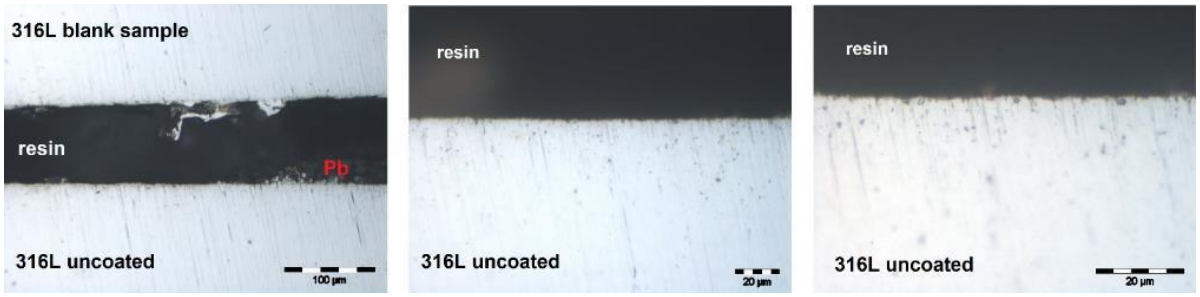

Fig. 7.15. *Cross section of an uncoated 316 L stainless steel sample tested for 500 hours in liquid lead at different size orders: X 200; X 500; X 1000.*

However, after 1000 hours of exposure to liquid lead, the uncoated sample shows corrosion in the matrix as shown in Figure 7.16. Penetration depths measured at several locations are between 2.7 µm and 7.3 µm.

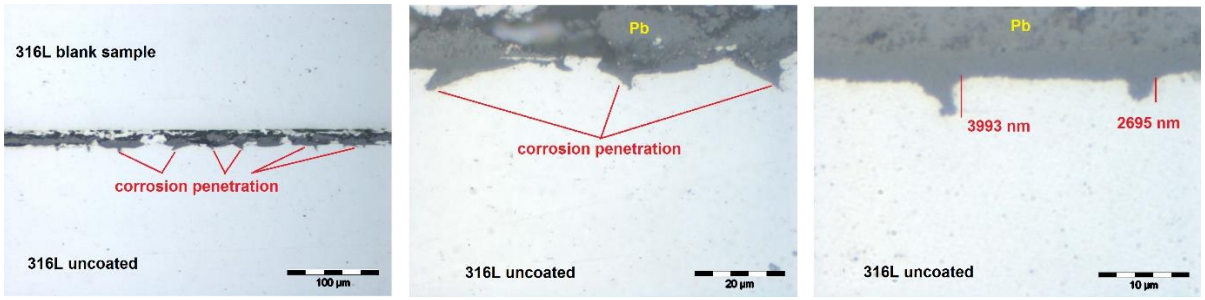

Fig. 7.16. *Cross section of an uncoated 316 L stainless steel sample tested for 1000 hours in liquid lead at different size orders: X 200; X 1000; X 2000.*

Figure 7.17 shows that after 500 hours of testing in liquid lead at 550°C, the 316L sample shell is still intact, adherent and compact. The coating thickness measured with an x2000 magnification microscope after the molten lead test was about 3.0 um for the interlayer and 5.2 um for the alumina layer.

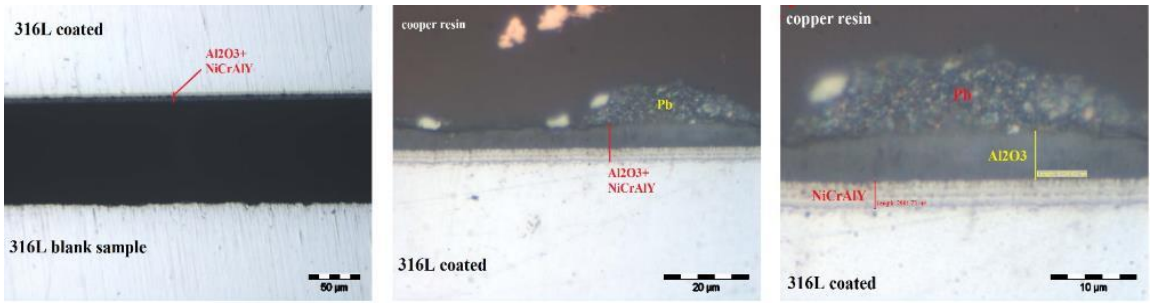

Fig. 7.17. *Cross section of a 316 L stainless steel coated specimen tested for 500 hours in liquid lead at different size orders: X 240; X 1000; X 2000.*

Even after 1000 hours of exposure to molten lead, the 316L coated sample still shows a continuous, intact, adherent and compact film, as shown in Figure 7.18. In this case, the thicknesses measured after the test were 3.1 μm for the NiCrAlY buffer layer and 5.2 for the Al_2O_3 layer.

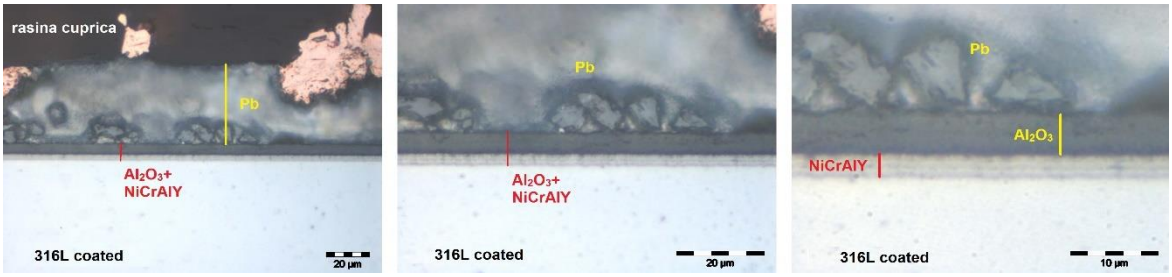

Fig. 7.18. *Cross section of a 316 L stainless steel coated specimen tested for 1000 hours in liquid lead at different size orders: X 500; X 1000; X 2000.*

Chapter 8

OBTAINING AND CHARACTERISING LAYERED AND MULTILAYERED OXIDE ARCHITECTURES OF THE TYPES: Acros (NiCrAlY) -Al_2O_3 - LZO - GZO – TiO_2, Al_2O_3, Al_2O_3, - LZO - GZO, Al_2O_3, - TiO_2, Al_2O_3, - LZO - GZO – TiO_2, ON 304 L STAINLESS STEEL SUBSTRATE BY THE EB-PVD METHOD

8.1. Obtaining experimental models of NiCrAlY- ZrO2 - LZO - GZO - TiO2 multilayer oxide architectures by EB-PVD method

In order to obtain multilayer oxide architectures of the type: acrosium (NiCrAlY) – Al_2O_3 - LZO - GZO -TiO_2, 304L stainless steel plates with dimensions of 30x50x2 mm were used as substrates, which were previously cleaned and degreased in an isopropyl alcohol/acetone bath, using ultrasound at the same time (Figure 3.9.).

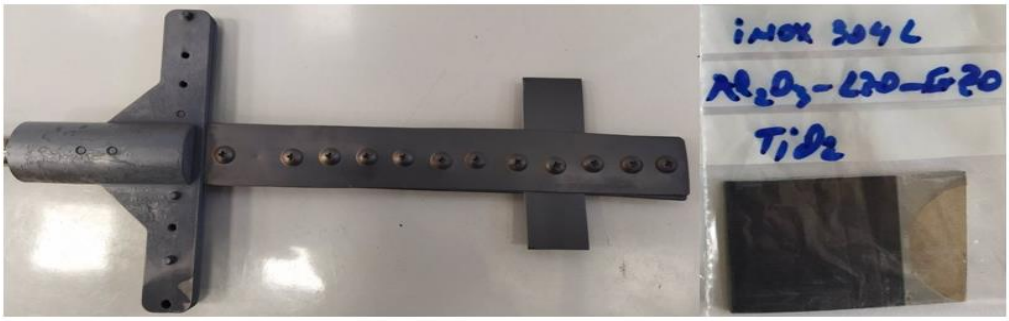

Fig. 8.7. *EB- PVD deposition samples of (NiCrAlY)- Al_2O_3 - LZO - GZO -TiO_2*

8.2. Characterization of multilayer oxide architectures obtained: EB- PVD acros (NiCrAlY) - ZrO2 - Ce - LZO - GZO -TiO_2 deposition samples on 304 L stainless steel substrate by EB-PVD method

For the characterization of the experimental multilayer oxide deposition patterns on 304L stainless steel substrate obtained by EB-PVD, a complex investigation methodology was established, by applying various analysis methods: SEM-EDS, scrach test, X-ray diffraction (XRD) and corrosion test.

Microstructural and microcompositional investigation was performed by scanning electron microscopy (SEM) and energy dispersive X-ray microanalysis (EDS) electron scanning FEI Qanta 250, Fig. 3.17. present in the analysis laboratory at IMNR. The morphological appearance corresponding to the samples developed on the 304L stainless steel support surface using the EB-PVD process are shown in Figure 8.8.

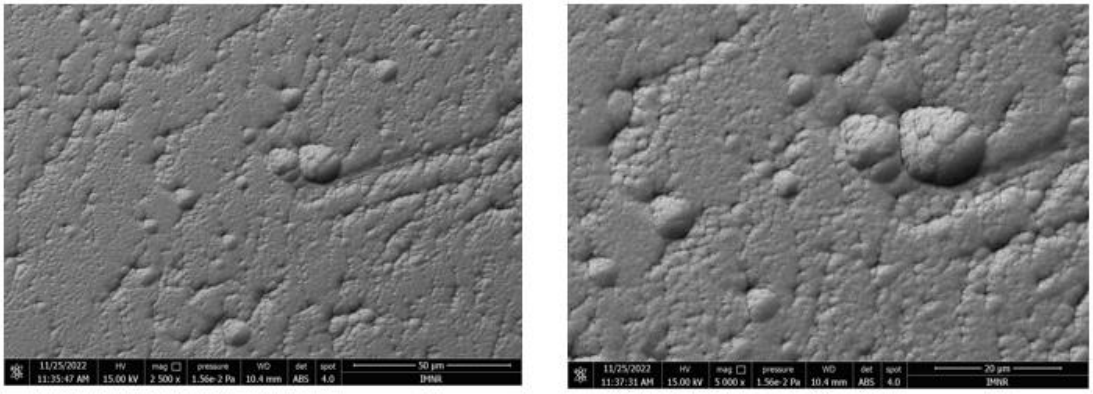

Fig. 8.8. *SEM image at (M=2500; 5,000 X) surface re-sampled magnifications for the (NiCrAlY)- Al_2O_3 - LZO - GZO -TiO_2 oxide material.*

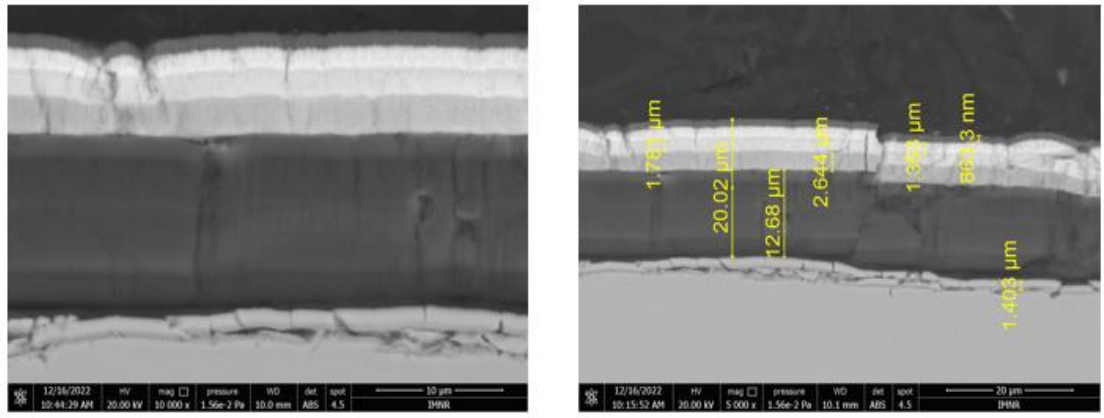

Fig. 8.10. *SEM images at magnifications (M=5000X; 10,000X) with measurements of the cross-sectionally re-sectioned deposited layers for the (NiCrAlY)- Al_2O_3 - LZO - GZO - TiO_2 oxide material.*

Acros (NiCrAlY) - Al $_2O_3$ - LZO - GZO -TiO_2 samples on 304L stainless steel substrate obtained by the EB-PVD process were evaluated by performing a scratch test. The test was carried out with a "NANOVEA Scratch Test" - scratch/adhesion tester: M0-M1250 conical 120 degrees 50 micrometers. The results are shown in Fig. 8.20.

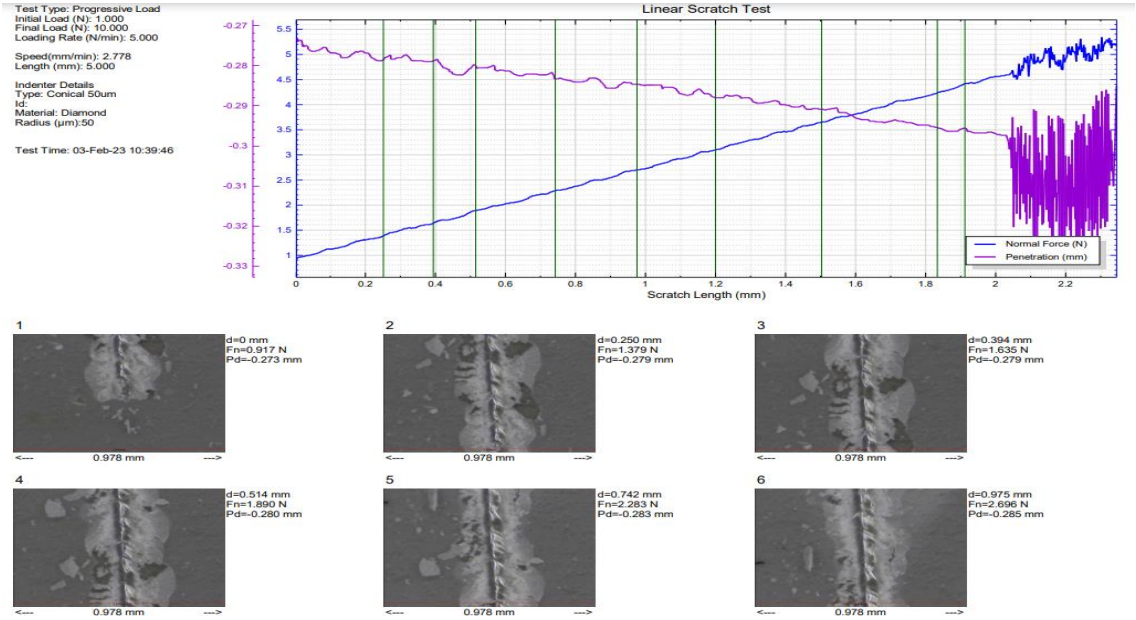

Fig. 8.12. *Adhesion test on the specimen performed on the (NiCrAlY)- Al_2O_3 - LZO - GZO -TiO_2 on 304L stainless steel substrate obtained by EB-PVD*

The friction graph in Figure 8.19. shows the data collected during scratching. During the progressive scratching process, an initial load of 1 N was increased in with load in steps of 5 N/min until the final load of 10 N was reached. The intermediate load was applied over a distance of 5 000 mm at a speed of 2.77 (mm/min). As the normal pressing force increased, the coating first peeled off cohesively and then adherently.

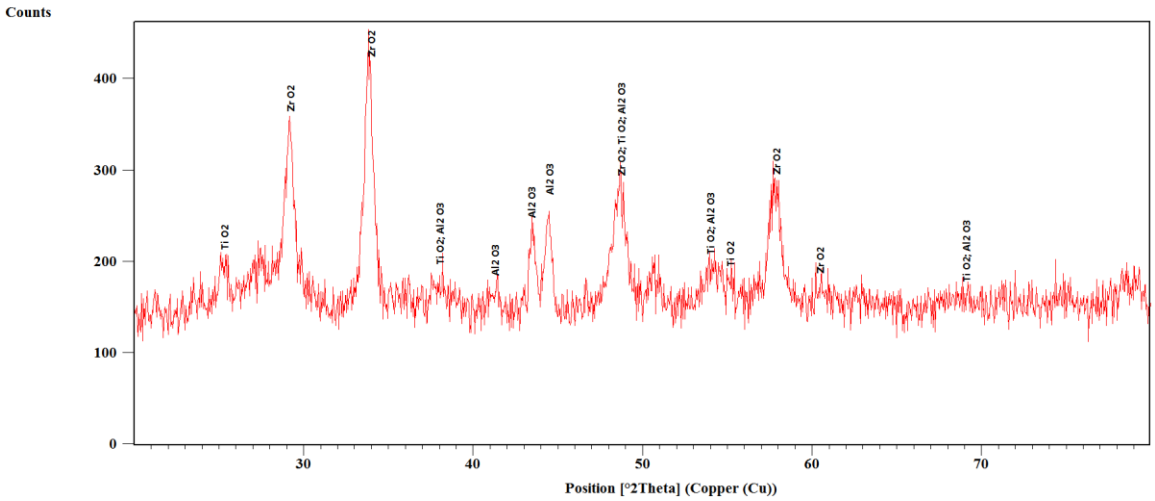

Fig. 8.13. *X-ray diffractogram of EB- PVD (NiCrAlY)- Al_2O_3 - LZO - GZO -TiO_2 sample*

The X-ray diffractogram analysis for the (NiCrAlY)- Al2O3 - LZO - GZO -TiO2 sample obtained by the EBPVD method is shown in Fig.8.13. According to these results, it is observed that OPR-doped ZrO2 has a tetragonal structure, whose positions are close to those specified in ICDD 04-007-2523. TiO2 has a tetragonal structure, whose positions are close to those specified in ICDD 01-071-1168. The layers were analysed under various angles of incidence to modify the ratio between the substrate and the deposited layer so, for both layers diffraction lines with low intensity were detected. It is therefore difficult to assess the exact nature of the phases formed.

8.11. Electrochemical corrosion resistance testing of Al_2O_3 - LZO - GZO – TiO_2, Al $_2O_3$, Al_2O_3 - LZO - GZO, Al $_2O_3$ – TiO_2, Al2O3 - LZO - GZO, Al_2O_3 – TiO_2, Al_2O_3- LZO - GZO – TiO_2 multilayer oxide architectures on 304 L stainless steel substrate by EB-PVD method

Electrochemical corrosion studies were carried out at room temperature in a flat corrosion cell (Figure 3.5), equipped with 3 electrodes: working electrode - material to be analysed,

exposed surface 16.9 cm2; reference electrode - Ag/AgCl in 3M KCl solution; counter electrode - 316 stainless steel. The 3 electrodes are coupled to a PGSTAT 128N Autolab potentiostat/galvanostat (Methrom) connected to a computer with NOVA 2.1 software. The electrolyte solution used was 1N H_2SO_4, according to ASTM G5-14 standard. [129]. The experiments were carried out after 60 minutes of immersion of the electrodes in the electrolyte solution studied.

The working procedure by which the experiments were conducted was linear polarization. This consists of determining the open-circuit working electrode potential (OCP), followed by linear sweep voltammetry (LSV), with a step profile, in the potential range -0.1 V ÷ +0.1 V with respect to the open-circuit potential, with a sweep rate of 0.001 V/s. Analysis of the corrosion process was performed by determining the following parameters from the Tafel curve:

- corrosion potential, Ecorr (V)

- corrosion current density, jcorr (A/cm2)

- corrosion rate (mm/year)

- polarisation resistance, Rp (Ω)

In this chapter of the PhD thesis the corrosion resistance of the following types of coatings on 304L stainless steel substrate was studied for the following samples:

- P_0 uncoated 304L stainless steel ;

- P_1 stainless steel 304L - acrosium (NiCrAlY) Al2O3 - LZO - GZO;

- P_2 stainless steel 304L - Al_2O_3

- P_3 stainless steel Al2O3 - LZO - GZO

- P_4 stainless steel - Al_2O_3 -TiO2

- P_5 stainless steel - Al_2O_3 - LZO - GZO-TiO2

The results obtained for the multilayer coatings compared to the uncoated substrate (304L stainless steel) are shown in Table 8.9.- 8.11. and Figure 8.35.

Table 8.9. *Corrosion process parameters in H_2SO_4 1N electrolyte solution*

Try	Ecorr, Obs (V)	jcorr (A/cm²)	icorr (A)	Corrosion rate (mm/years)	Polarisation resistance (Ω)
P1	0.391443041	2.80647E-07	2.80647E-07	0.003261105	92848.46098
P2	0.398658304	5.98088E-08	5.98088E-08	0.000694975	435683.0441
P3	-0.098377575	5.07636E-07	5.07636E-07	0.005898703	51331.39086
P4	-0.069364591	9.89478E-07	9.89478E-07	0.011497675	26334.76909
P0	-0.057472335	6.89247E-05	6.89247E-05	0.800900917	378.0600316
P5	-0.198099606	6.16312E-06	6.16312E-06	0.071615075	4228.001224

Table 8.10. *Samples with best corrosion resistance (lowest corrosion rate)*

Try	Corrosion rate (mm/years)
P2	0.000694975
P1	0.003261105
P3	0.005898703
P4	0.011497675
P5	0.071615075
P0	0.800900917

Table 8.11. *Samples with the best resistance to polyspray*

Try	Polarisation resistance (Ω)
P0	378.0600316
P5	4228.001224
P4	26334.76909
P3	51331.39086
P1	92848.46098
P2	435683.0441

Figure 8.35. *shows the Tafel curves in 1N H2SO4 electrolyte solution for samples P0, P1, P2, P3, P4, P5.*

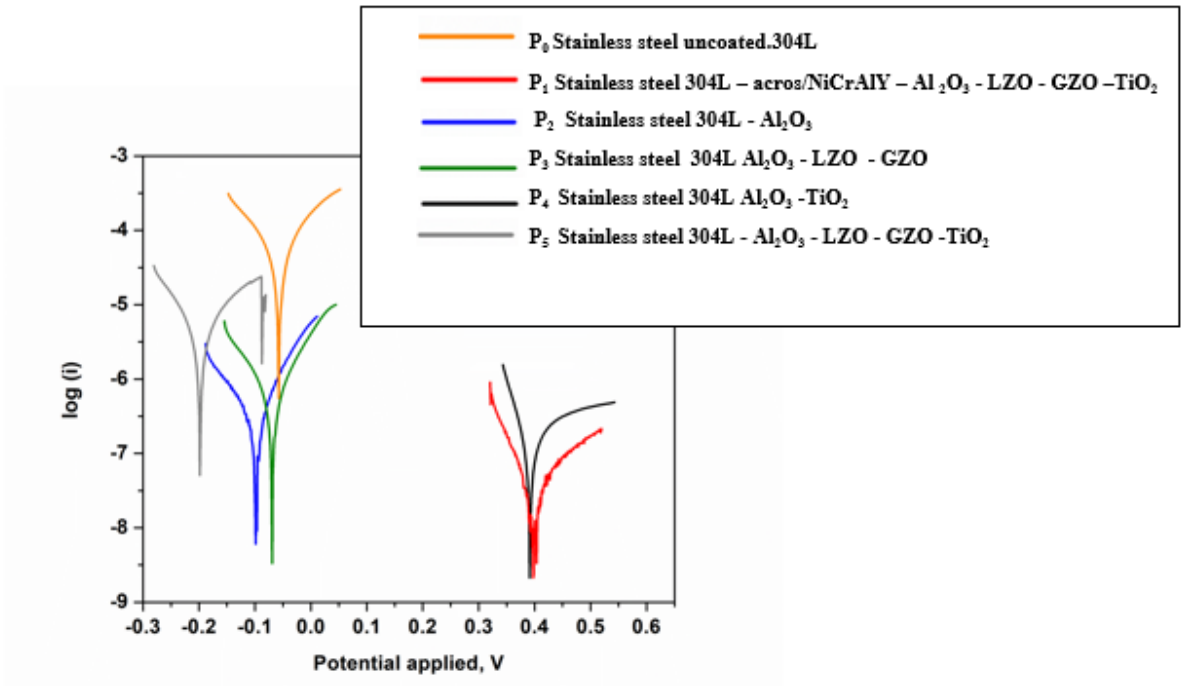

Fig. 8.35. *Tafel curve in 1N H_2SO_4 electrolyte solution for samples P0, P1, P2, P3, P4, P5.*

Calculation of corrosion rates requires determination of corrosion currents. When the mechanisms of the corrosion reaction are known, the corrosion currents can be calculated from the analysis of the slopes of the Tafel curves. To perform Tafel analysis, it is necessary to have information about the electrode surface area, equivalent weight (ratio of the atomic mass of the corroding metal to the number of electrons exchanged in the anodic dissolution reaction) and material density. From the slopes of the Tafel curves we obtain the corrosion rate and the polarization resistance. The higher the polarization resistance (Rp), the more corrosion resistant the material under study and the lower the corrosion rate over time.

Chapter 9

FINAL CONCLUSIONS, ORIGINAL CONTRIBUTIONS AND FUTURE PERSPECTIVES

Final conclusions

In the framework of the PhD thesis "Advanced research on obtaining thin films with high corrosion resistance under extreme conditions by PVD methods", advanced multilayer materials with programmed architecture capable of responding to thermo-chemical corrosion

stresses were obtained with potential applications in the development of new components for thermal equipment working under extreme environmental conditions.

Based on the studies carried out in the literature, new oxide layer and multilayer architectures of Al_2O_3, ZrO_2 and TiO_2, capable of responding to thermo-chemical corrosion stresses, were obtained in the PhD thesis. The coatings were obtained using the EB-PVD combinatorial electron beam vacuum deposition method, with a particular focus on the development of new components for thermal equipment operating under extreme environmental conditions.

Thus the objectives, research methodology and experimental design were formulated. In order to achieve the main objective of the PhD thesis, the following was considered:

- Specific selection of the required materials used as substrate- 304L and 316L stainless steel substrate;
- Design of oxide layer and multilayer materials and architectures for extreme temperature and corrosion conditions by predictive thermodynamic calculations using specialized software as well as literature data;
- A hydrothermal computer system was used to obtain nanocrystalline ZrO_2 powder doped with rare earth oxides;
- Thermodynamic modeling of hydrothermal synthesis processes of Y_2O_3 - doped ZrO_2 was performed;
- Thermodynamic modelling of hydrothermal synthesis processes of ZrO_2 doped with ZrO28%MCe_2O_3 was performed;
- Thermodynamic modelling of hydrothermal synthesis processes of $La_2Zr_2O_7$ doped ZrO_2 was performed;
- For the characterization of nanostructured powders obtained by hydrothermal synthesis at INCDMNR-IMNR, a complex methodology was established to determine the chemical and structural composition by applying various analytical methods: ICP-OES, DSC-TG, XRD, SEM-EDS.
- A series of experimental solutions using specific materials for corrosion resistance enhancement based on Al_2O_3, ZrO_2 and TiO_2 were studied by the EB-PVD combinatorial method;

- Multilayer oxide architectures such as Al_2O_3; ZrO_2 doped with Y_2O_3; ZrO_2 doped with C_2O_3; $La_2Zr_2O_7$ on austenitic 316L stainless steel substrate were obtained by EB-PVD method;
- The proposed concept was demonstrated by corrosion testing of oxide architectures obtained in NaCl electrolyte solution of different concentrations, i.e.0.06M, 0.2M, 0.4M and 0.6M, according to ASTM G61-86 (Reapproved 2003);
- Multilayer oxide architectures such as Al_2O_3, ZrO_2 doped with rare earth oxides (CeO_2; Nd_2O_3; La_2O_3; GdO_3) were obtained on austenitic 304L stainless steel substrate by EB-PVD method;
- The efficiency of the oxide layers obtained was performed by corrosion testing in 1N H_2SO_4 solution;
- Experimental models of Al_2O_3 type oxide layer samples on 316L austenitic stainless steel substrate were obtained by the EB-PVD combinatorial method;
- The proposed concept was demonstrated by performing corrosion tests in molten lead for 500 h and 1000 h at 550°C. at ICN Pitesti;
- Obtaining layered and multilayered oxide architectures such as ZrO_2Ce - LZO - GZO - TiO_2, Al_2O_3 - LZO - GZO, Al_2O_3, Al_2O_3 -TiO_2, Al_2O_3 - LZO - GZO -TiO_2, Al_2O_3 - YSZ - LZO- GZO on austenitic 304L stainless steel substrate by EB-PVD method;
- The efficiency of the oxide layers obtained was performed by corrosion testing in 1N H $_2SO_4$ solution. The experiments were carried out after 60 minutes of immersion of the electrodes in the electrolyte solution studied.
- Elaboration of a plan of investigation and characterization of the experimental patterns of oxide layer and multilayer deposits obtained by EB-PVD by applying various methods of analysis: SEM - EDS, Scrach test, X-ray diffraction.

Personal contributions

- Complex study carried out in the literature on how to obtain multilayer oxide coatings by the EBPVD method with the aim of identifying some elements of originality in the scientific approach to obtain Al_2O_3, ZrO_2 thin layers doped with rare earth oxides (La, Ga, Y) and TiO_2 capable of responding to the demands of thermo-chemical corrosion

with potential applications in the development of new components for thermal equipment working in extreme environmental conditions.

- The use of specialised software for predictive thermodynamic calculations that have been programmed architectures of materials with high potential for chemical-physical stability;
- Obtaining new layer and multilayer architectures using NiCrAlY as a needle layer by total or partial substitution of some critical materials (W, Mo, Nb, Ta) currently widely used in specific applications in energetics, able to reduce the working temperature in the contact zone with the metal interface to values below the degradation temperature;
- Obtaining by hydrothermal synthesis of proposed nanostructured powders based on doped ZrO_2 following the influence of synthesis parameters (temperature, time, pH) on the composition and microstructure of the powders;
- Establishment of the research methodology scheme in order to obtain oxide layer and multilayer architectures using austenitic 304L and 316L stainless steel as substrate on the influence of thermo-chemical corrosion process;
- Evaporation under vacuum and controlled atmosphere conditions of ceramic oxide materials to obtain oxide architectures using electron beam evaporation method EBPVD;
- Combinatorial EB-PVD method to obtain novel innovative architectures with programmed functional gradient for corrosion conditions in NaCl electrolyte solution of different concentrations, i.e. 0.06M, 0.2M, 0.4M and 0.6M.
- Combinatorial EB-PVD method to obtain new innovative architectures with programmed functional gradient for corrosion conditions in 1N H_2SO_4 electrolyte solution.
- Combinatorial EB-PVD method to obtain new innovative architectures with functional gradient programmed for extreme corrosion conditions in molten lead.

Future perspectives

- Continue research by developing new types of protective coatings for applications involving intense temperature and corrosion processes by testing the developed

coatings in conditions as close as possible to real-life conditions in specific energy applications;

- Further research by obtaining new nanostructured materials based on doped ZrO2 through synthesis and characterisation of advanced materials for extreme environmental conditions.
- Validate rapid methods for the analysis of advanced materials in the form of multilayer coatings, offering new analysis and characterisation services to enterprise partners and research centres.
- Based on the studies performed using the EBPVD deposition method, further research can be carried out on the deposition of new thin layers that can be used for various applications such as thermal barrier coatings in the protection of metallic components, which are used in aero and land-based gas turbines.

BIBLIOGRAPHY

[1] F. Silva, R. Martinho, R. Alexandre, A. Baptista, Wear Resistance of TiAlSiN Thin Coatings, Journal of Nanoscience and Nanotechnology, Volume 12, Number 12, December 2012, pp. 9094-9101(8).

[2] F. Silva, R. Martinho, R. Alexandre, A. Baptista, Increasing the wear resistance of molds for injection of glass fiber reinforced plastics, j.wear (2011) 01.074.

[3] F. Silva, R. Martinho, M. Andrade, A. Baptista, R. Alexandre, Improving the wear resistance of moulds for the injection of Glass Fibre- Reinforced Plastics Using PVD Coating: A Comparative Study, Coatings (2017) 7, 28.

[4] D. A. Jameel, Thin Film Deposition Processes, International Journal of Modern Physics and Applications Vol. 1, No. 4, pp. 193-199, 2015.

[5] J. Thirumalai, Introductory Chapter: The Prominence of Thin Film Science in Technological Scale, http://dx.doi.org/10.5772/67201.

[6] A. Baptista, F. Silva, J. Porteiro, J. Míguez and G. Pinto, Sputtering Physical Vapour Deposition (PVD) Coatings: A Critical Review on Process Improvement
and Market Trend Demands, Coatings, 8, 402; doi:10.3390/coatings8110402, 2018.

[7] M. Urbina et.al; The theologies and strategies for the development of novel material systems and coatings for applications in extreme environments: a critical review' Manufacturing Rev. 5, 9 (2018).

[8] Mattox, Donald M. "The Foundations of Vacuum Coating Technology" Noyes Publications (2003).

[9] Mattox, Donald M. and Vivivenne, Harwood Mattox (editors) "50 Years Of Vacuum Coating Technology and the Growth of the Society of Vacuum Coaters", Society of Vacuum Coaters (2007).

[10] H. Soonmin, S. A. Vanalakar, Ahmed Galal and Vidya Nand Singh, A review of nanostructured thin films for gas sensing and corrosion protection, Mediterranean Journal of Chemistry, 7(6), 433-451, 2019.

[11] P. A. Savale, Physical Vapor Deposition (PVD) Methods for Synthesis of Thin Films: A Comparative Study, Archives of Applied Science Research, 8 (5):1-8, 2016

[12] M.C. Lovell, A.J. Avery and M.W. Vernon, Physical Properties of Materials, Van Nostrand Reinhold, England, (1976).

[13] MELLES GRIOT technical manual. (www.mellesgriot.com).

[14] Westwood, William D. "Sputter Deposition", AVS Education Committee Book Series, AVS Vol. 2 (2003).

[15] Markus Back, Investigation of the properties of thin films grown via sputtering and resistive thermal evaporation, Uppsala University, [2015]

[16] M. Lorenz, R. MSR. 25 years of pulsed laser deposition. J. Phys. D. Appl. Phys.; 47:030301–030303. DOI: 10.1088/0022-3727/47/3/030301, 2014.

[17] D. Lowndes, D. Geoghegan, P.AA Rouleau CM. Synthesis of novel thin film materials by pulsed laser deposition. Science; 273(5277):898–903. DOI: 10.1126/ science.273.5277.898, 1996.

[18] M.NR Ashfold, F. Claeyssens, GM Fuge, SJ Henley. Pulsed laser ablation and deposition of thin films. Chem. Soc. Rev;33(1):23–31. DOI: 10.1039/B207644F, 2004.

[19] L. Lynds, B.R. Weinberger, DM Potrepka, GG. Peterson, MP Lindsay. High temperature superconducting thin films: The physics of pulsed laser ablation. Physica C;159(1– 2):61–69. DOI: 10.1016/0921-4534(89)90104-4 Advance Deposition Techniques for Thin Film and Coating doi.org/10.5772/65702 147, 1989.

[20] RE. Russo, X Mao, JJ Gonzalez, V Zorba, J. Yoo. Laser ablation in analytical chemistry. Anal. Chem.;85(13):6162–6177. DOI: 10.1021/ac4005327, 2013.

[21] Geyer TJ, Weimer WA. Parametric effects on plasma emission produced during excimer laser ablation of YBa2Cu3O7-x. Appl. Spectros.;44(10):1659–1664. DOI: 10.1366/ 0003702904417454, 1990.

[22] W. A. Bryant, J. Mater. Sci. 12, 1285, 1977.

[23] R. N. Ghoshtagore, J. Electrochem. Soc. 125, 110, 1978.

[24] T. Suntola, Thin Solid Films 216, 84, 1992.

[25] R. R. Chamberlin and J. S. Skarman, J. Electrochem. Soc. 113, 86, 1966.

[26] C. J. Brinker, A. J. Hurd, G. C. Frye, K. J. Ward and CS. Ashley, J. Non-Cryst. Solids 121, 294, 1990.

[27] C. C. Chen, M. M. Nasrallah and H. U. Anderson, J. Electrochem. Soc. 140, 3555, 1993.

[28] C. J. Brinker, G. C. Frye, AJ. Hurd and CS. Ashley, Thin Solid Films 201, 97, 1991.

[29] Olayinka Oluwatosin Abegunde, Esther Titilayo Akinlabi, Oluseyi Philip Oladijo, Stephen Akinlabi1 and Albert Uchenna Ude ; Overview of thin film
deposition techniques; AIMS Materials Science, 6(2): 174–199.

[30] Olayinka Oluwatosin Abegunde, Overview of thin film deposition techniques, AIMS Materials Science, 6(2): 174–199.

[28] Muñoz-Rojas D, MacManus-Driscoll J. Spatial atmospheric atomic layer deposition: a new laboratory and industrial tool for low-cost photovoltaics. Mater Horiz.; 1:314–320, 2014.

[31] Pardon Nyamukamba, Omobola Okoh, Henry Mungondori, Raymond Taziwa and Simcelile Zinya; Synthetic Methods for Titanium Dioxide Nanoparticles: A Review; doi 10.5772/intechopen.75425 (2018).

[32] Livage J, Ganguli D. Sol-gel electrochromic coatings and devices: A review. Sol. Ener. Mater. Sol. Cells.2001;68:365–381. DOI: 10.1016/S0927- 0248(00)00369-X

[33] Tjong SC, Chen H. Nanocrystalline materials and coatings. Mater. Sci. Eng. R. 2004;45(1–2):1–88. DOI: 10.1016/j.mser.2004.07.001

[34] Brinker CJ, Scherer GW. Sol-Gel Science. San Diego: Academic Press; 1990.

[35] Review Article: Withdrawing a solid from a bath: how much liquid is coated? E. Rio, & F. Boulogne.

[36] Mitzi, D.B., Kosbar, L.L., Murray, C.E., Copel, M. and Atzali, A., “High mobility ultrathin semiconducting films prepared by spin coating”, Nature, 428, 299- 303, 2004.

[37] Flow of a Viscous Liquid on a Rotating Disk, E. G. Alfred et al., J. Appl. Phys. (29), 858–862 (1958).

[38] Characteristics of resist films produced by spinning, D. Meyerhofer, J. Appl. Phys. (49), 3993–3997 (1978).

[39] An Investigation of the Thickness Variation of Spun-on Thin Films Commonly Associated wtih the Semiconductor Industry, J. W. Daughton, J. Electrochem. Soc. (129), 173–179 (1982).

[40] Dynamics of polymer film formation during spin coating, Y. Mouhamad, J. Appl. Phys. (116), 123513 (2014).

[41] Yagi, K. Kakizawa, K. Murakami and S. Kaneko, J. Ceram. Soc. Jap., 102 (1994)

[42] A. I. Y. Tok, F.Y. C. Boey, X. L Zhao, Journal of Materials Processing Technology 178, 270, 2006.

[43] A. Aoki and G. Nogami, J. Electrochem. Soc., 143, 191. C. S. Huang, C. S. Tao and C. H. Lee, J. Electrochem. Soc., 144 (1997) 3556, 1996.

[44] Hyun-Suk Kim, Chang Sool Kim, Sun-Geon Kim, J. of Non- Crystalline Solids 352, 2204, 2006.

[45] P. S. Patil, E. A. Ennaoui, C. D. Lokhande, M. Muller, M. Giersig, K. Diesner and H. Tributsch, Thin Solid Films, 310, 57, 1997.

[46] C. H. Chem., A. A. J. Buysman, E. M. Kelder and J. Schoonman, Solid State Ionics, 80, 1, 1995.

[47] R. N. Singh, J. F. Koenig, G. Poillerat and P. Chartier, J. Electroanal. Chem., 314, 214, 1991.

DISSEMINATION OF RESULTS

Scientific papers presented at national and international conferences

- Radu-Robert Piticescu, Mircea Corban, Arcadii Sobetkii, **Laurențiu Moșinoiu**, Gheorghe Matache, A. Paraschiv, ELECTRON BEAM - PHYSICAL VAPOR DEPOSITION (EB-PVD) OF THERMAL BARRIER COATING (TBC) FOR TURBINE BLADES, 1st International Conference on Emerging Technologies in Materials Engineering EmergeMAT and 4th International Workshop on Materials under Extreme Conditions SUPERMAT 14-16 November 2018, Bucharest, Romania
- Arcadii Sobetkii, **Laurențiu Moșinoiu**, Mircea Corban, Victor Manoliu, Mihai Boțan, G. Ionescu, Bogdan Vasile, R. Trusca, A. Surdu, Radu Robert Piticescu, Zirconium perowskites as novel materials for high temperature coatings developed through combinatorial EB-PVD deposition technology, 2nd International Conference on Emerging Technologies in Materials Engineering EmergeMAT, 06-08 noiembrie 2019, București, România

- **Laurențiu Moșinoiu,** Arcadii Sobețkii, Mircea Corban, Matei Alexandru Cristian, Daniel Petrescu, Review On The Design Of A Multilayer Material: Nicraly - Al_2O_3 Deposited By Eb-Pvd Process On Austenitic 316L Stainless Steel Support, With Applications In Nuclear Industry, International Conference "Emerging Technologies In Emergemat Materials Engineering" 29-30 October, Bucharest, 2020.
- **Laurențiu Moșinoiu,** Arcadii Sobețkii,Radu Piticescu, Mircea Corban, Daniel Petrescu, "Microstructural aspects of Cr E-beam deposition on Zr alloy support - Zircaloy-4, with applications in the nuclear industry", International Conference "Emerging Technologies In Emergemat Materials Engineering" 4-5 November, Bucharest, 2021.
- **Laurențiu Moșinoiu,** Arcadii Sobețkii, Radu Piticescu, Mircea Corban, Alexandru Cristian Matei, Aspects about the corrosion in molten Pb of stainless steel 316 L coated by EB-PVD with thin films of: NiCrAlY andAl_2O_3 intended for applications in nuclear energy, 5th International Conference Emerging Technologies in Materials Engineering.
- Arcadii Sobețkii, **Laurențiu Moșinoiu**, Mircea Corban, Thin film deposition of HEO (High Entropy Oxides) materials by PVD methods and characterization for potential use in SOFC (Solid Oxide Fuel Cell) applications, 5th International Conference Emerging Technologies in Materials Engineering.
- DESIGN, SYNTHESIS AND CHARACTERIZATION OF EB-PVD THERMAL BARRIER COATINGS BASED ON RARE EARTH ZIRCONATES FOR AEROSPACE APPLICATIONS R. R.Piticescu, A. Sobetkii, A. E. Slobozeanu, A. Ghiță, M. Corban, **L. F. Moșinoiu,** C. Bogdanescu, M. Botan, 5th International Conference Emerging Technologies in Materials Engineering.

Articles published in specialist journals

Articles published in ISI-listed journals

- Sobetkii A., **Mosinoiu L.,** Paraschiv A.,Corban M., Piticescu R.R., Matache G., „Microstructural aspects of the protective ceramic coatings applied on the surfaces of refractory alloys produced by additive manufacturing", Manufacturing Review, Open Access, Volume 72020 Article number 2020031, DOI: 10.1051/mfreview/2020031.

- **Laurentiu Florin MOSINOIU**, Cristian PREDESCU, Radu Robert PITICESCU, Mircea CORBAN, Arcadii SOBETKII, Alexandru Cristian MATEI, Laura Madalina CURSARU, Albert Ioan TUDOR, The influence of multylayer Al_2O_3 and CeO_2 doped ZrO_2 coatings on 316L autenitic steel corrosion in H_2SO_4 solution, U.P.B. Sci. Bull., Series B, Vol. 84, Iss. 1, 2022 ISSN 1454-2331.
- **Laurentiu Mosinoiu**, Arcadii Sobetkii, Mircea Corban, Radu Robert Piticescu, Nicoleta Zarnescu Ivan, Laura Madalina Cursaru, THE INFLUENCE OF THIN MULTI-LAYER OXIDE COATINGS MADE BY EB-PVD, ON THE CORROSION OF 316 L STAINLESS STEEL – Journal of Science and Arts, Volume 22, Issue1, pp. 197-210, 2022.